Bar-Ilan University

Department of Physics

Light induced SIT

Neria Oshry

Submitted in partial fulfillment of the requirements for

M.Sc Degree, in the Bar Ilan University.

Ramat Gan, Israel 2016

Bar-Ilan University

Department of Physics

Light induced SIT

Neria Oshry

Submitted in partial fulfillment of the requirements for

M.Sc Degree in the, Bar Ilan University.

Ramat Gan, Israel 2016

This work was carried out under the supervision of

Prof. Aviad Frydman

Department of Physics, Bar-Ilan University.

Table of content

Abstract

The Superconductor-Insulator Transition (SIT) in thin films is an important phenomenon, which is in the front of condensed matter research today. It is considered as a classical example of a quantum phase transition, in which a system transits from an insulating state to a superconducting state at zero temperature. Most of the SIT research focuses on the quantum critical regime, since in this regime the behavior of the films is non-trivial. Though there has been a large research effort, both experiment and theory, much of the physics is not so understood, in particular, the nature of the insulating state.

One of the proposed models to explain some of the features observed in these systems is the “emergent granularity”, which invokes the presence of granular behavior despite the fact that the films exhibit continuous morphology. Electronically, experiments have shown that this granularity is manifested by SC islands surrounded by an insulating sea. InO films, which undergo the SIT, are one example for this unique type of systems.

Far from the SIT, deep in the insulating side, experiments on such films have shown an existence of an electron-glass behavior, which is characterized by a slow relaxation of the conductivity after pushing the system out of equilibrium.

In this work, we present an experiment aimed at studying the influence of light on InO samples at different degrees of disorder from a deep insulating state to a superconducting state, achieved by thermal annealing. For each stage, resistance versus temperature (R(T)) was initially measured, after which light was shone for few hours, and then turned off followed by a second R(T) measurement. Resistance as a function of time was measured during the whole process.

Our main findings are the following:

1. Light causes an increase in conductance, which possesses a logarithmic dependence with time.
2. After turning off the light, this increase persists for a relatively long time with a very slow relaxation that also follows a logarithmic behavior.
3. The improvement of conductivity leads to an enhancement of the coupling between SC islands, resulting in pushing the system deeper towards the SC side. One of the outcomes is the so called "light induced SIT", in which a sample with a degree of disorder which is slightly above the SIT, crosses the SIT and becomes a superconductor, by just shining light on it.
4. Light did not change the morphology of the samples but rather the electronic properties.

Combining all results together, we suggest a model, in which the insulating regions between SC grains behave as an electron glass. By shining light on the system, the "normal" electrons are excited to higher "meta-stable" energy levels, resulting an increase of the coupling between the SC islands. This is manifested as an increase in the conductivity of the sample. Close to the SIT, this conductance increase can transit a sample, which is initially insulating, to a superconducting state, due to generation of global phase coherence between the SC grains. In the SC side, it can increase the critical temperature of a superconductor and

Our work adds a new dimension of measurements, which not only provides further evidence for emergent granularity but also presents qualitative information on the characteristics of the material in between these SC grains, and may lead to a new type of SIT. This work has a significant impact on the investigation of disordered superconductors and opens a window for additional measurements, which can provide more information about the properties of these films.

1. Introduction

1.1. Anderson localization

Perfect ordered crystalline systems obey Bloch theorem, which asserts that the wave function of electrons in ordered crystals is extended and periodical. In reality, every crystalline sample has imperfections in its structure such as dislocations, fractures or alien atoms. The presence of imperfections results in the breakdown of the Bloch mechanism. While at low degree of disorder this manifests itself as a small perturbation, leading to small corrections to the conductivity (weak localization), at high level of disorder the effect is much more dramatic.

In 1958, Anderson showed [1] that in a presence of sufficiently large disorder, the paths of the electrons are annihilated leading to a breakdown of Bloch functions and localization of the electronic wave function, which in turn leads to insulating behavior. In this limit, the electrons are confined to small sites so the wave function exponentially decays with a characteristic length, ξ, the localization length:

$$\left|\psi(r)\right| = \psi_0 e^{-\frac{|r-r_0|}{\xi}} \tag{1.1}$$

Mott further expanded [2] on conductivity in disorder systems. He showed that in localized systems, there are two contributions to electronic transport from one localized state to another, one is tunnelling to a nearby unoccupied state and the other is jumping to higher (or lower) energetic state by absorbing (or emitting) a phonon. This process of tunnelling accompanied by phonons is known as "hopping". The probability of this process decays exponentially both with the distance between the two sites, i and j, and with the energy difference between the initial level and the final level of the electron, and is given by the following expression:

(1.2) $$p \propto e^{-\frac{r_{ij}}{\xi}-\frac{\varepsilon_{ij}}{k_B T}}$$

where r_{ij} is the distance between the sites and ε_{ij} is the energy difference between them.

Mott also postulated that the density of states, N(E), is constant in the vicinity of the Fermi energy and under this assumption he showed that the resistance follows a broken exponent relation with temperature:

(1.3) $$R(T) = R_0 e^{-\left(\frac{T_0}{T}\right)^{\alpha}}$$

where $T_0 \propto \frac{1}{N(E_F)\cdot\xi^d}$, and α the characteristic exponent which depends on the dimensionality of the system, d: $\alpha = \frac{1}{d+1}$.

In other words, in 2D: $R(T) \propto e^{-\left(\frac{T_0}{T}\right)^{\frac{1}{3}}}$ and in 3D: $R(T) \propto e^{-\left(\frac{T_0}{T}\right)^{\frac{1}{4}}}$.

Efros and Shklovskii [3] showed that the assumption of constant density of states is incorrect when taking into account Coulomb interactions. Assuming a ground state in which all electrons occupy states below the Fermi energy and the states above it are vacant, excitation of an electron from energy E_i below E_f to energy E_j above it requires overcoming the Coulomb interaction between the electron and the hole left behind (e_{ij}). In the ground state, the total energy of this process satisfies the inequality:

(1.4) $$\Delta E = E_j - E_i - e_{ij} > 0$$

If the density of states is constant, there will always be an E_j that is close enough to E_f, so that the Coulomb interaction is stronger than the excitation energy $E_j - E_i$, thus breaking the above inequality, and producing a state with energy lower than the ground state. Thus we get a contradiction. This leads to the so called "Coulomb gap" in the density of states. The density of states

cannot be constant, it depends on dimension and close to Fermi energy, behaves like: $N(E) \propto \left(E - E_f\right)^{d-1}$, so that:

(1.5)
$$\mathrm{N_{2D}(E)} \propto |\mathrm{E} - \mathrm{E_f}|$$
$$N_{3D}(E) \propto \left(E - E_f\right)^2$$

These changes are also reflected in the characteristic exponent α of the transport equation (1.3), leading to a dimensionality-independent constant $\alpha = \frac{1}{2}$. i.e.,

(1.6)
$$R(T) = R_0 e^{-\left(\frac{T_0}{T}\right)^{\frac{1}{2}}}$$

T_0 also needs to be recalculated considering the updated DOS. Efros and Shklovskii found that it is proportional to the Coulomb interaction in a localization site, i.e. $T_0 = \frac{e^2}{\epsilon\xi}$, where ϵ is the dielectric constant.

1.2. Percolation theory

As discussed above, the conductivity of a disordered system is determined by hopping of the electrons amongst localized sites with exponential decay with distance and energy. The probability of a hop decreases exponentially with disorder so that the calculation of the conductivity by mean field approximation becomes somewhat problematic. A useful way to treat these systems is by the percolation theory. The basic concept is based on a lattice model, in which every site acts as lattice point.

Bond percolation problem

Considering only nearest neighbors, in the percolation theory one defines a probability *p* for bonds to be connected and a probability *1 – p* to be non-connected. With increasing *p*, more connecting bonds are formed and the lattice points evolve to clusters. These clusters grow progressively with *p* until

at some critical percolation probability p_c, an infinite cluster from one edge to the other is formed and the conductivity becomes macroscopic, as demonstrated in Fig. 1.1.

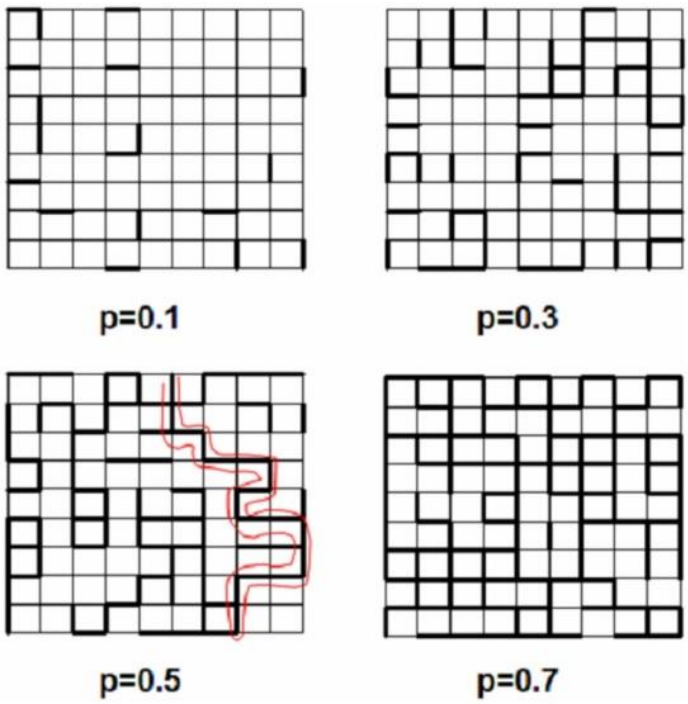

FIG. 1.1: Bond percolation on a square lattice (thin lines) for different values of the probability *p*. Thick lines represents the suitable bonds for the value of *p*. The red curve marks the shortest percolation path at $p=p_c=0.5$, taken from [4].

The value of p_c varies from lattice to lattice and has a strong dependence on the number of nearest neighbors, z, and on the dimensionality of the sample, d. An approximation given by Shante and Kirkpatrick [5] sets:

$$p_c = \frac{d}{z(d-1)} \tag{1.7}$$

Random lattice

In a disordered metal, the localized sites do not form an ordered lattice but rather randomly distributed sites in the system. Hence, it demands different treatment. In random lattices, each site generates bonds with any other site in the sample, while the bond strength is inverse proportional to its length, so that a network is formed. To sketch the network, one uses the so-called “r-

percolation process", starting with the shortest bonds and gradually increasing the length up to the bonds with a macroscopic length. Since each site has infinite number of bonds, P is defined as the average number of bonds per site. Since each pair of bonds has different length, one defines the correlation function $C(r)$ as the probability for two bonds at distance r to belong to the same finite cluster. These definitions give rise to a new length-scale L_p, or the correlation length, which is the average length between two critical bonds in the cluster:

$$L_p^{\,2} = \frac{\sum_r r^2 C(r)}{\sum_r C(r)} \tag{1.8}$$

In the vicinity of P_c, it diverges with:

$$L_P \propto \left|P - P_c\right|^{-\nu} \tag{1.9}$$

where ν is the critical exponent.

Resistors network

Ambegaoker, Langer and Halperin [6] developed the r-percolation model for conductivity in strongly disordered systems, in which connections between localized sites are considered as resistors, presenting a complex network as sketched in Fig. 1.2. Since the resistance is given by:

$$R = R_0 \exp\left\{\frac{r_{ij}}{\xi} + \frac{\varepsilon_{ij}}{k_B T}\right\}$$

the resistors strengths depends on the "space-energy" distance between sites, where high resistivity is represented by a long distance which is equivalent to a low rate of hopping, and low resistivity is represented by a short distance which is equivalent to high rate of hopping. In a highly disorder system the values of resistances vary over many orders of magnitude, thus one can define the critical resistor, R_c, as the lowest resistor which allows an infinite cluster,

i.e. the maximum resistance for percolation conductivity. Because of the large resistance span, R_c is not only critical resistance but rather the characteristic resistance of the system since it is the higher resistance which participates in the backbone cluster.

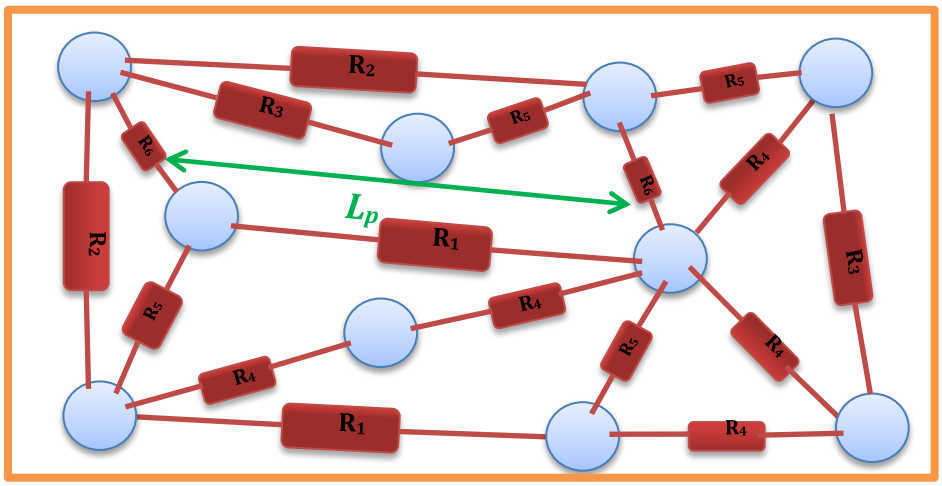

FIG. 1.2: A sketch of resistors network, according to ALH model. In this sketch $R_c = R_6$ and L_p is the distance between two R_6 resistors (green arrow).

In this mechanism, the percolation length L_p is defined as the "space-energy" distance between two critical resistances.

As a consequence, the length of the sample, L, has a nontrivial impact on the conductivity of the system. At $L \gg L_p$ the system is in the macroscopic limit, in which fluctuations are adequately averaged, leading a "nominal conductivity" (same samples show same conductivity). However, at $L \sim L_p$ the system is within the mesoscopic scale, in which the number of percolation paths decreases, results in mesoscopic fluctuations leading the so called "sample to sample conductivity" (same samples show different conductivity).

Another important quantity is the relation between the localization length and the percolation length, $\frac{\xi}{L_p}$, which determines the strength of the backbone, since ξ is equivalent to the width of the current path. $\xi \ll L_p$ leads to a diluted thin current, meaning that most of the system is a dead wood and not participate in the backbone cluster.

1.3. Electron glass

One of the outcomes of strong electron-electron interactions and disorder in metal films is the presence of glassy behavior, namely the inability to reach a thermodynamic equilibrium in a reasonable experimental time.

In nature, a number of glasses have been identified such as spin glass, vortices glass, and the common window glass, in which a glass is obtained (usually in amorphous materials) below the temperature of glass, or T_g, below which the system transits from a liquid to a glassy state. These glassy systems are characterized by a slow relaxation to equilibrium after an excitation.

Based on theoretical arguments, Davies *et al.* [7] suggested 30 years ago that a highly disordered electronic system may demonstrates glassy behavior, since the combination of electron-electron interactions and high disorder leads to a wide distribution of energies, which is reflected in wide local hopping probability and relaxation times. In these electornic disordered systems, termed the "Electron glass" (EG), the glassy objects are believed to be the conducting electrons. In EG, the disorder leads to a random potential in the energy space, which can be described as a many valley landscape in the configuration space, as sketched in Fig 1.3. The barriers are explored in accordance with the temperature of the system.

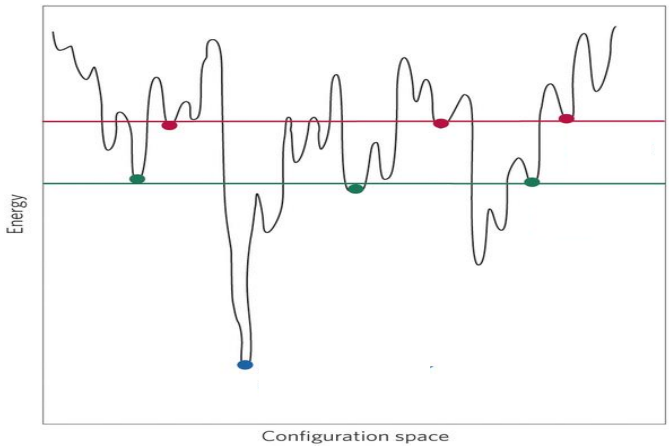

FIG. 1.3: A sketch of the configuration space of a glassy state. The state of the system depends on the temperature, when different temperature explores different basins, in which the system resides for a long time before relaxation to a lower state. Taken from [8].

The transport of electrons is expressed as very slow motion from a local basin to a lower basin through the barriers, since they remain trapped in each basin for a relatively long time.

The EG systems are characterized by a change of the conductance following a change in the external conditions, such as temperature or electric field. As a results of an external perturbation, energy is inserted to the system leading a change in the potential of the configuration space, and thus pushing the system out of equilibrium to an excited state, after which collective glassy transitions of many electrons take place in order to return to equilibrium.

This process was observed experimentally few decades ago in InO [9], granular Al films [10] and discontinuous gold films [11], by measurement of conductance versus time. Similar to some glassy systems [12], the conductance in EG systems shows a clear logarithmic decay with time after an excitation. However, in contrast to other glasses, this behavior was shown to be independent of temperature. Hence, until recently, the EG was believed to be a quantum glass, i.e. governed by quantum tunneling through barriers in the configuration space, rather than by thermal activation above them.

However, lately it was shown by Eisenbach *et al.* [13], that at moderate temperature, the glassy dynamics becomes dependent of temperature and the motion speeds up with temperature, where crossing a barrier is controlled by an Arrhenius law. At sufficiently low temperatures, the thermal activation is insufficient and the quantum-mechanical processes are dominant. These quantum-mechanical transitions are inherently slow, after which is reflected in a very slow relaxation of conductivity towards equilibrium.

Fundamentally, the EG systems are characterized by few main parameters:

1.3.1. Logarithmic relaxation

As mentioned above, pushing a system out of equilibrium by an external perturbation leads to an increase of the conductivity, followed by a slow

relaxation of conductivity. In an EG, these relaxations follow a logarithmic behavior. Thus, time dependent conductance of an EG can be described by:

$$G(t) = G_{ex} - A\log\left(\frac{t}{t_{\min}}\right) \tag{1.10}$$

where t_{min} is a microscopic time, related to the time required for a single electron rearrangement, G_{ex} is the conductance of the excited state, and A is a system dependent constant.

There are several ways to generate a slow relaxation by excitation. Ovadyahu *et al.* [14] suggest three different methods, as depicted in Fig 1.4. The first, presented in the upper panel, is by biasing the sample with a large electric field F between the source and the drain contacts. The second, presented in the middle panel, is by exposing the sample to a light source for a short period (marked by the arrows). The third, presented in the bottom panel, is by changing a gate voltage in a MOSFET geometry, at which the sample was equilibrating.

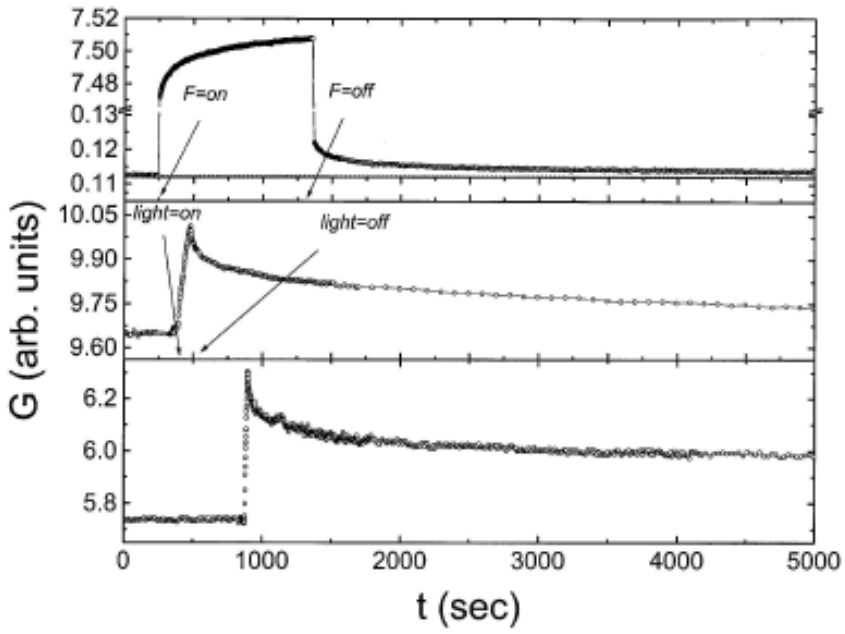

FIG. 1.4: *Top:* Conductance versus time during the application of a large source-drain electric field. *Middle:* Conductance versus time during and after a short exposure (marked by the arrows) to a burst of IR light. *Bottom:* Conductance versus time of a gate voltage change from $V_g = -50V$ to $V_g = 50V$ at $t=900s$. Taken from [14].

Fig. 1.5 presents the logarithmic slopes of EG as measured by Z. Ovadyahu [9] immediately after an excitation period of high source drain electric field. In this figure, the relaxation slopes were taken for a 52.5MΩ sample with a thickness of 52Å under various electric fields *F*.

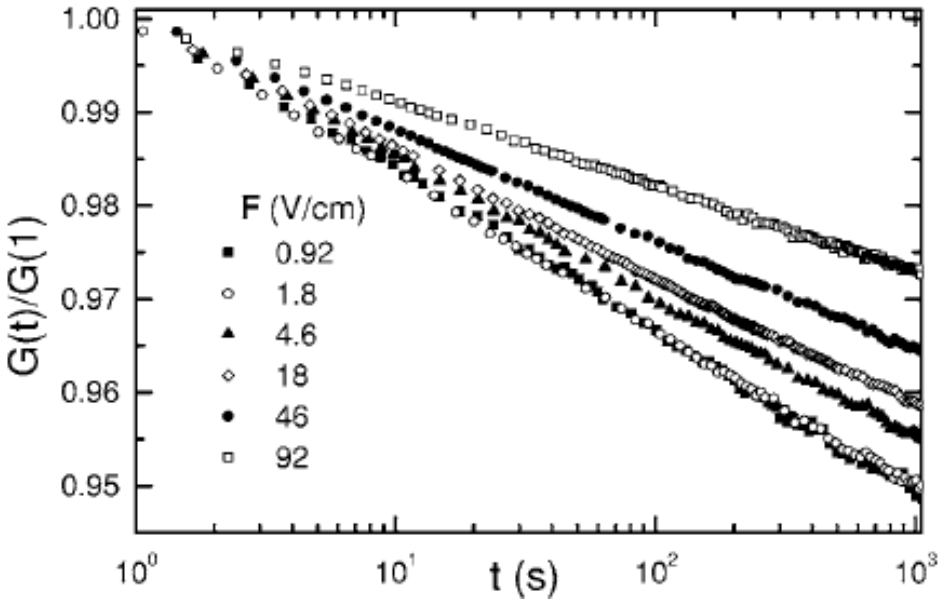

FIG. 1.5: Normalized conductance vs. time on log scale of the 52.5MΩ sample with a thickness of 52Å, measured under various electric fields *F*, exhibits a logarithmic relaxation.

In conclusion, EG is a non-trivial phenomenon, which has been gaining more attention in recent years, in disordered electronic systems, and expressed mainly by a slow relaxation to equilibrium.

1.4. The Superconductor – Insulator Transition

One of the consequences of the localization theory is the influence of disorder and localization on superconducting systems. Anderson [15] and Abrikosov and Gor'kov [16] showed separately that weak disorder does not prevent superconductivity in a system. However, experimental work showed that strong enough disorder destroys superconductivity, thus turning the system to an insulator. These results have given rise to the pronounced research on the so called: “superconductor – insulator transition (SIT)”.

The SIT is characterized by a quantum phase transition from a superconducting system to an insulating system in the two-dimensional limit.

A classic phase transition is governed by thermal fluctuations and is characterized by a critical temperature, above which the system is in one phase, and below it – the system transits to other phase. An example for this type of phase transition is superconductivity, in which the system transits from a normal state to a superconducting state at a critical temperature (T_c).

In recent years, there is a lot of interest in a different type of phase transitions, i.e. quantum-phase transitions (QPT), in which the transition occurs at T=0 and is a function of a tuning parameter, g, that is non-thermal and controlled by quantum fluctuations. At T=0, the phase transition occurs at a quantum critical point (QCP), $g = g_c$, while at T>0, a quantum critical regime is generated around g_c, as sketched in Fig. 1.6.

The SIT is an example for a quantum phase transition since the transition from superconductor (SC) to insulator occurs at T=0 and depends on various non-thermal tuning parameters such as: thickness, magnetic field, disorder level, composition, etc.

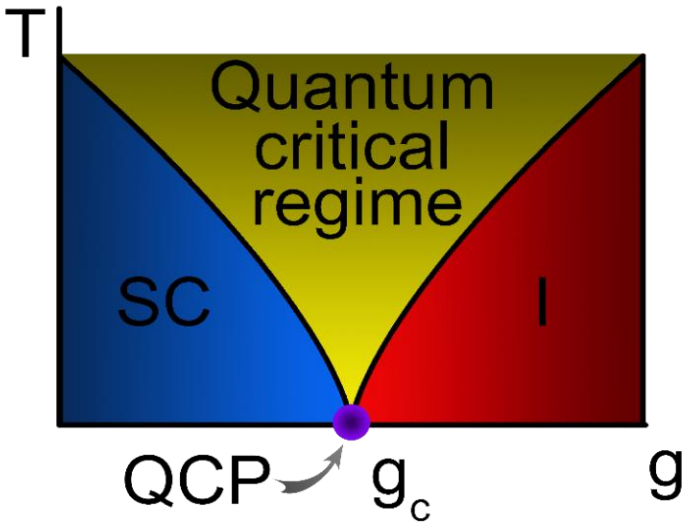

FIG. 1.6: An illustration of a quantum phase as a function of a tuning parameter g, where g_c is the critical point at T=0. At T>0, there is a quantum critical regime with a temperature dependent width.

For example, if g is the degree of disorder, at sufficiently low level of disorder and low but finite temperature, the film is a superconductor. With increasing disorder level, superconductivity is progressively suppressed until the system crosses the quantum critical regime, and the film becoming increasingly insulating [17].

Nowadays, the research of the SIT focuses on the physics of films in the quantum critical regime, since in this regime the behavior of the films is special and a number of non-trivial effects are observed, such as disorder giant magneto-resistance peak [18] and unique I-V curves [19].

Basically, there are two main models of the SIT which are derived from two approaches. A superconducting state is described by a macroscopic wave function:

$$\psi = \psi_0 e^{i\theta}, \tag{1.11}$$

where ψ_0 is the amplitude of the order parameter which is proportional to the density of cooper pairs, and θ is the phase of the state. Suppression of the superconducting state can be obtained by two ways: (1) destroying cooper pairing, (2) perturbing the phase correlation. As a consequence, it is necessary to distinguish between two main types of SITs, which manifest themselves in homogeneous films versus granular films. Fig. 1.7 presents results of two different types of Sn films, homogeneous (a) and granular discontinuous (b). For each type, R(T) curves were taken for different thicknesses. The upper curves represent thinner films and the lower curves thicker films. The SIT occurs in both samples. However, in the homogeneous films (Fig. 1.7(a)) the transition is sharp with a well-defined T_c, which increases as the film thickens. On the other hand, in the granular films (Fig. 1.7(b)) the transition is broad with a slope becoming broader as the film becomes thinner.

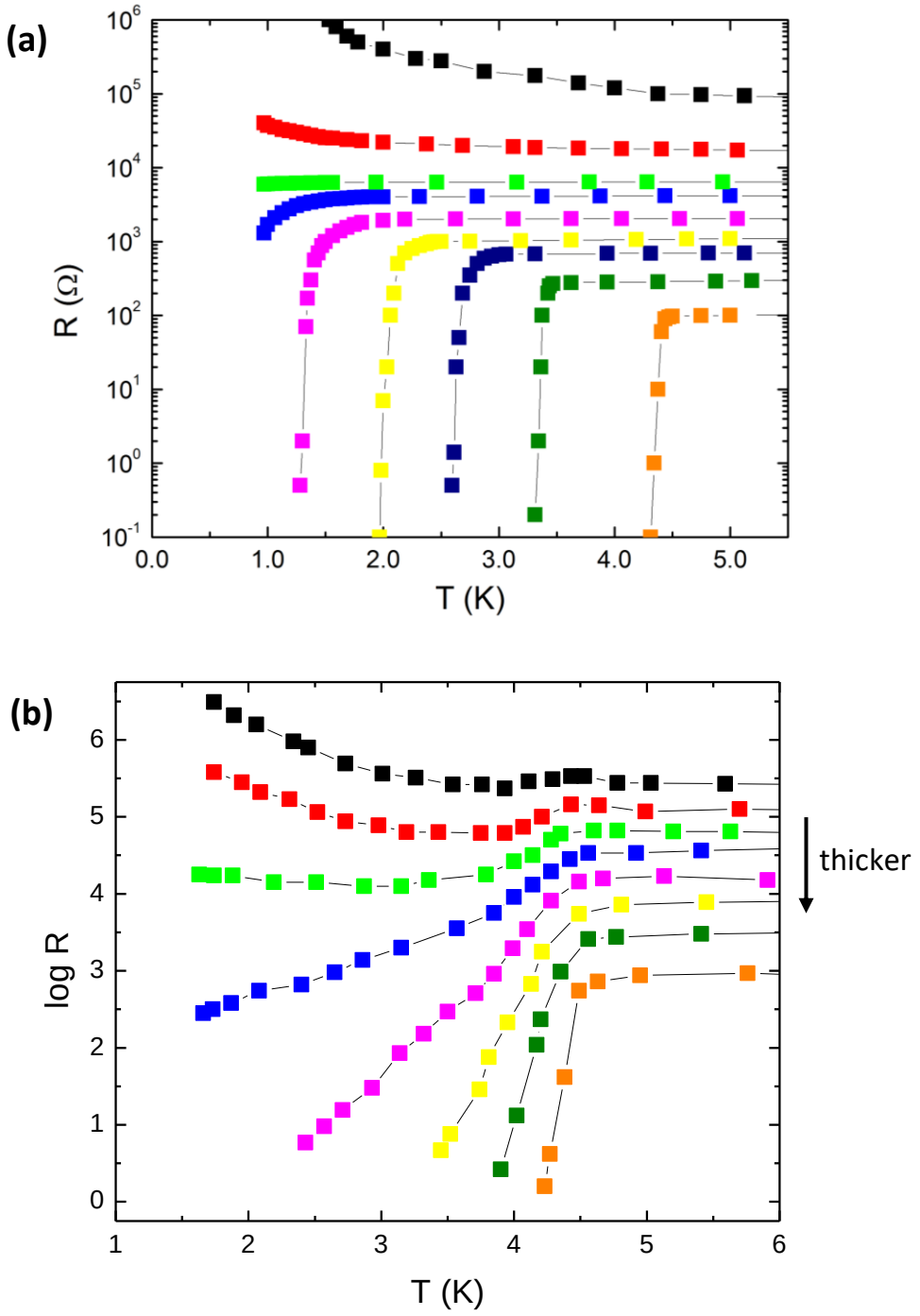

FIG. 1.7: (a) An example for a homogeneous Sn film and its R(T) curve as a function thickness. **(b)** An example for a granular Sn film and its R(T) curve as a function of thickness, taken from [20].

This distinction between the two types of SIT seen in Fig. 1.7 is due to the physical differences between these two types, as explained in the following paragraphs.

1.4.1. Homogeneous films

The first type of SIT occurs in homogeneous films (Fig. 1.7(a)), such as the Tin layer evaporated on thin wetting layer of Germanium, fabricated on a silicon substrate (see AFM image presented in Fig. 1.8). In this type of metals, the morphology is continuous thus the phase is expected to be coherent throughout the entire film. Hence, the superconducting properties depend on the amplitude of the order parameter which is determined by the density of Cooper pairs $\left(N_c = 2|\psi_0|^2\right)$.

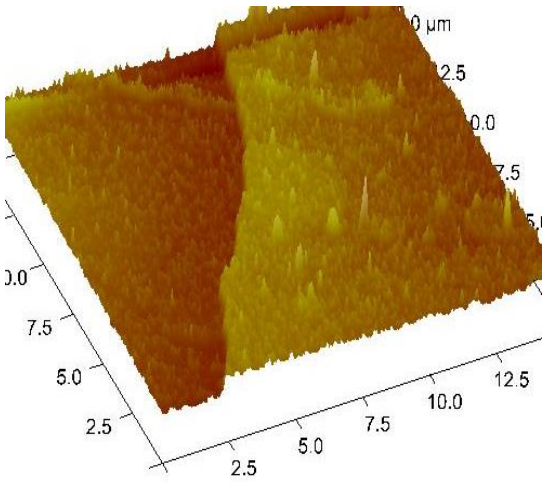

FIG. 1.8: An AFM image (atomic force microscope) of a step of 1nm homogeneous Tin film on Germanium layer.

This corresponds to the so called “fermionic model” of the SIT that was first proposed by Maekawa [21], further developed by Takaji *et al.* [22] and later by Finkel'stein [23]. It is based on electron-electron interactions. In ordered systems, the Coulomb interaction is screened by a balance between the background's positive charge and the electron's negative charge. This screening allows Cooper pairing which is required for superconductivity. As mentioned above, disorder leads to localization of the electronic wave functions. This leads to reduction of the screening so the coulomb repulsion becomes more dominant, and thus suppresses the pairing of the electrons.

The dimension of the samples affects unequivocally the disorder level. In 3D film, the influence of disorder is less significant because the thickness of the film adds electronic paths to the electrons and they can flow through the sample despite the presence of disorder. Disorder in ultra-thin films (2D) has a much larger influence on the transport of the electrons because of the absence of the thickness freedom. Accordingly, decreasing the thickness of the film is equivalent to increasing the disorder level.

Fig. 1.7(a) demonstrates that in this case increasing the thickness of a film decreases the effective disorder, and accordingly increases the T_c due to the enhancement of cooper pairing.

1.4.2. Granular films

The second type of SIT occurs in discontinuous granular films (Fig. 1.7(b)), such as granular Tin (see an AFM image presented in Fig. 1.9). In this type of samples, the SC film is not-continuous and grains act as potential wells for the electrons, so the wave function and the energy levels are localized in the grains. Although a grain itself can be a perfect superconductor, it may not "speak" to other grains because of absence of phase correlation. Therefore, suppression of superconductivity is achieved by fluctuations of the phase (θ).

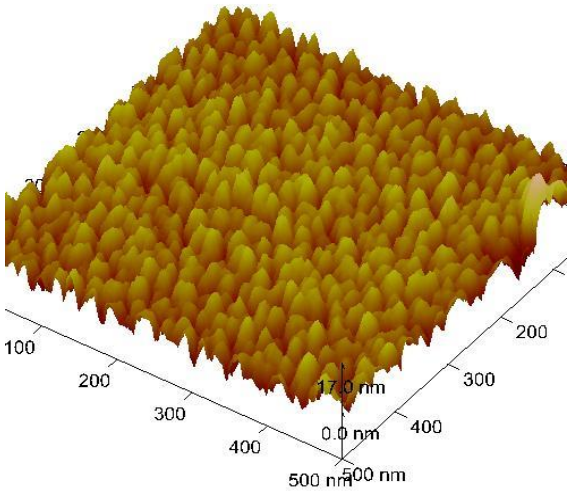

FIG. 1.9: An AFM image of a granular Tin layer with a thickness of 2nm.

This is in accordance with "bosonic model" of the SIT [24], in which the conductivity is based on Cooper pairs tunneling. Basically, Cooper pairs are localized in the grains. In order to generate superconductivity, they must hop from one grain to another via Josephson tunneling depending on the Josephson energy E_J. However, in order to enter the grain, Cooper pairs must overcome the charging energy of the grain, E_C, that is inversely proportional to the capacitance of the grain, C ($E_C = \frac{2e^2}{C}$). The ratio between these energies $\mu = \frac{E_C}{E_J}$ determines whether the system is superconducting or insulating.

For high μ, the charging energy is higher than the Josephson energy and Cooper pairs cannot hop between grains. Hence, they are localized in the initial grains, resulting in the system being a "boson insulator". With lowering μ, the probability of hoping increases thus inducing correlation between grains. It evolves progressively with gradually decreasing μ until at the QCP, phase correlation percolates across the film and the system becomes a superconductor. In this regime, superconductivity is weak due to reduced phase correlation, and the resistance does not drop sharply to zero, as presented in Fig. 1.7(b). Further decreasing of μ enhances the correlation, which in turn sharpens the slope.

This mechanism defines two important critical temperatures. One is T_p, the mean field temperature of the superconducting state of each grain i.e. the temperature in which Cooper pairs are generated in the grains, and the other is T_ϕ, a macroscopic T_c which is the temperature below which phase correlation is achieved throughout the entire sample and the resistance drops to zero. It can be seen in Fig. 1.7(b) that all curves have a kink at the same temperature, which is $T_p = 4.3K$. T_p is constant since it is the temperature of the bulk inside the grains. However, the zero resistance state occurs at a much smaller temperature. The requirement of global phase coherence defines a lower critical temperature than the pair breaking T_c of the grains.

An interesting conclusion of this model is the existence of Cooper pairs in the insulating side of the SIT. Indeed, traces of superconductivity have been observed experimentally. One example is the R(T) of Fig. 1.7(a), in which the upper curves in the insulator also change slope at the bulk T_c (around 4.5K). Likewise, tunneling experiments, like those conducted by Barber *et al.* [25], have proven existence of an energy gap of the bulk even in the insulating side.

In conclusion, as opposed to homogeneous films, in which the superconductivity (SC) is suppressed due to the braking of cooper pairs, in granular films, the SC is suppressed due to the perturbation of phase correlation between the grains, and therefore the SC transition is not sharp but broad, depending on the thickness or coupling.

1.4.3. Disorder induced granularity

A third type of SIT superconductors is a class of disordered composite films such as amorphous indium oxide (a-InO), titanium nitride (TiN), niobium nitride (NbN), etc. While these films are morphologically homogeneous, they show signs of electrical granularity, reflected in unexpected results in several experiments. This electrical behavior can be classified as "disorder-induced granularity".

Disorder-induced granularity is depicted as a mixture of superconducting and normal state regions across the film. The theory behind this granularity was largely developed by Ghosal *et al.* [26]. They used an attractive Hubbard model with random potential on each site and by numerical methods showed that in highly disordered systems the macroscopic superconducting state becomes limited to locally correlated sites with size ξ (the coherence length), in which superconducting islands are surrounded by insulating regions.

The evolution of the SIT according to this model is illustrated in Fig. 1.10. 1.10(a) represents the situation in of the insulating side, in which SC islands are separated by insulating states (the green lines). With decreasing disorder-level, the correlation between the SC regions grows while breaking the insulating bonds, up to the QCP (1.10(b)) in which the last bond is broken, leading to a formation of a SC path across the sample which brings the sample to a superconducting state (1.10(c)).

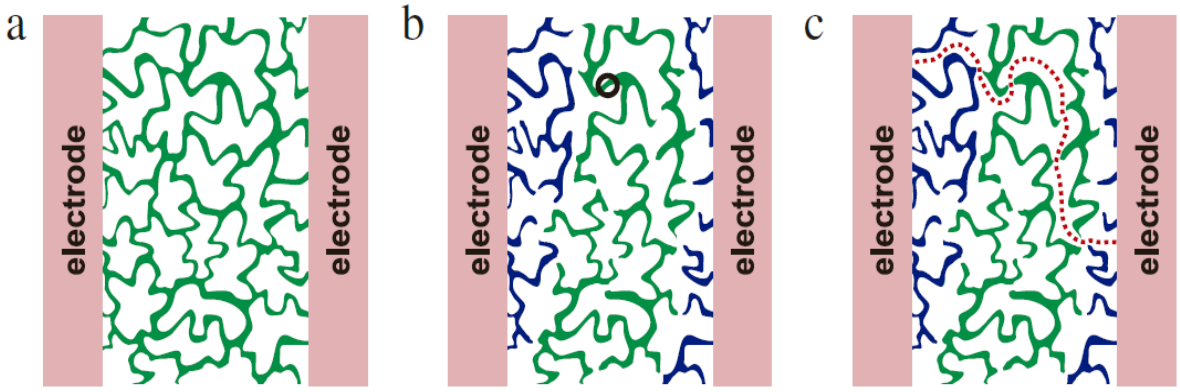

FIG. 1.10: A sketch of the SIT process according to emergent granularity theory is described above **(a)** Insulating state: SC regions bonded by insulating regions *(green lines)*. **(b)** QCP: The critical bond *(black circled bond)*, which is the last bond that prevents SC path. **(c)** Superconducting state: SC path is created across the sample *(dotted line)*, taken from [19].

Later on, Bouadim *et al.* [27] calculated the density of states by quantum Monte Carlo methods and predicted the existence of a SC "pseudo gap" above T_c and in the insulator, as showed in Fig. 1.11(a).

An experimental realization of this was demonstrated by Sherman *et al.* [28]. They conducted tunneling measurements on a pair of a-InO films, one superconducting (*S1)* and one insulating (*I*), and extracted the density of states as depicted in Fig. 1.11(b). The most substantial result is that despite the fact that sample *S1* is a strong superconductor and sample *I* is a strong insulator, they both have a similar SC energy gap.

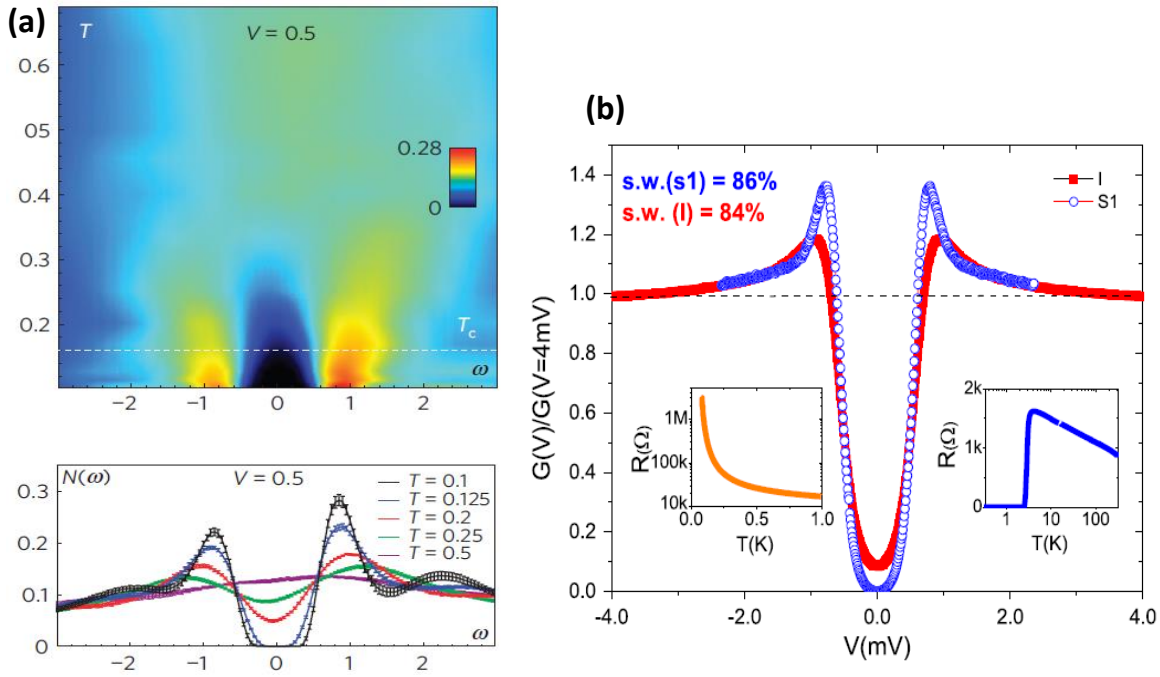

FIG. 1.11: The existence of pseudo gap in Anderson insulators, **(a)** Density of states according to Bouadim's prediction and its representative spectra along 5 different cuts of temperature, taken from [27] **(b)** Tunneling density of states of both samples I *(red squares)* and S1 *(blue circles)* that were taken at 1 K and zero magnetic field. Insets: R(T) measurements of sample I *(left)* and sample S1 *(right)*. Taken from [28].

In conclusion, even though the a-InO films are morphologically homogeneous, they may possess granular behavior due to the fact that strong disorder generate emergent electric granularity even in a morphologically ordered material.

2. Experimental

2.1. Indium Oxide films

Stoichiometric In_2O_3 is an insulator. When deposited on a sapphire substrate using e-beam evaporation, as sketched in Fig. 2.1, some of the oxygen atoms are released from the film and vacancies are generated, resulting in a continuous amorphous InO film with a certain oxygen deficit $q = 3 - x$ [28]. The resistance of the film depends on the number of vacancies (since vacancies act as electron donors), which in turn depends on the bled oxygen pressure in the chamber during the deposition process. Hence, one can control the resistance of the deposited film by tuning the oxygen pressure level. The SEM image of the film presented in Fig. 2.2 shows that the sample is continuous.

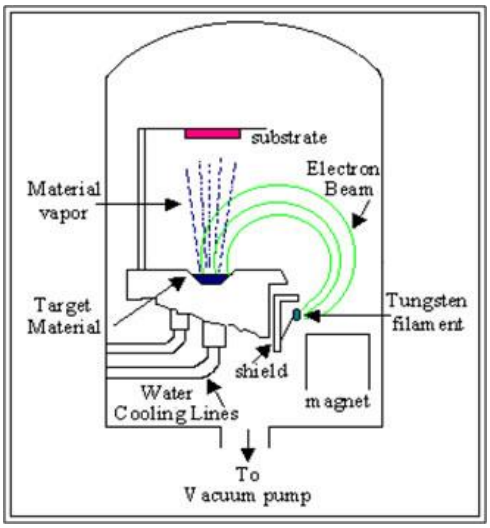

FIG. 2.1: A sketch of the deposition process in the chamber.

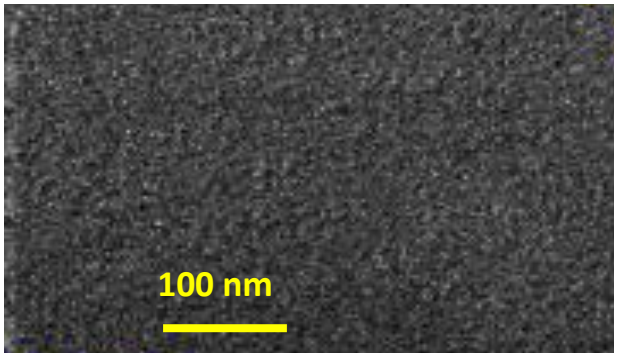

FIG. 2.2: A surface of a-InO film, imaged by a Scanning Electron Microscope (SEM).

The resistivity of the film can be also varied after the deposition by thermal annealing at temperatures of T < 80°C. Annealing in a vacuum reduces the disorder, leading a decrease in resistivity.

In our work, the samples underwent many stages of annealing in vacuum at 60-65°C, which led to different levels of disorder through the SIT. For each stage, resistance and temperature measurements were taken, as will be detailed below.

2.2. Preparation of films

The samples in this work were fabricated on a sapphire substrate, in two stages. First, gold contacts were deposited on the substrate, forming an empty strip of 0.8 mm in the middle by mask. Then, using a shaddow mask, an InO film of 5x0.8 mm was deposited in the middle, leading to the desired effective area, as sketched in Fig. 2.3. The accurate dimension were measured by a microscope and found to be 0.64*0.78 mm, leading to a geometry of be 1.22 squares.

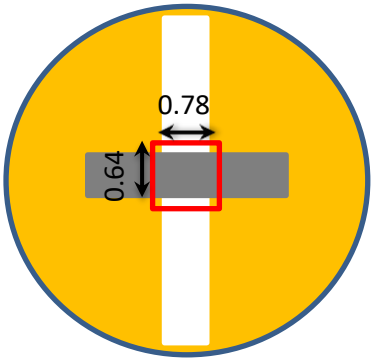

FIG. 2.3: A sketch of the sample. An amorphous InO_x film *(gray)* on gold contacts *(yellowed regions)* forms a desired film in the center *(red rectangle surrounded region)*.

The InO e-beam deposition was conducted in varied oxygen pressures in the range between $1\text{-}5 \cdot 10^{-5}\ torr$ and at a deposition rate of 1.2 $\mathring{A}/\mathrm{sec}$. The thickness of the samples was 30 nm.

2.3. Measurements

Using optics at low temperatures requires utilization of an optical cryostat, i.e. a cryostat with windows that can reach cryogenic temperatures.

We use an RC-100 cryostat of "CRYO industries". It consists of an external vacuum chamber, which is necessary for preventing heat transport during the cooling of the system, a hollow insert for liquid helium, a sample holder, which is thermally attached to the helium, and a shield for blocking radiation (see sketch in Fig. 2.4).

To support cryogenic temperatures, the system is operated by the helium flow method, in which liquid helium is transferred to the cryostat and helium gas pumped out simultaneously. This results in reduction of the surface tension of the liquid and decreasing of the temperature to below 4.2K. Thereby, the cryostat reaches a base temperature of 1.3-1.6K.

FIG. 2.4: The RC-100 cryostat. The right panel is an overall view of the system. The left panel is a picture of the optical path through the cryostat, while the sample is placed on the copper ring.

In order to decrease thermal radiation as much as possible and ensure that the sample temperature will reach the base T, we fabricated a metal disk, which is

thermally attached to the shield, so the effective aperture is of the order of the sample dimensions. We also placed a window sapphire on the metal ring for filtering the unwanted radiation, as presented in Fig. 2.4.

For the light beam, we used a helium-neon laser with wavelength of 632.8 nm, which is equivalent to an energy of 1.96 eV, and with power of 6mW. In order to focus the incident light, we placed a lens at a distance of focal length from the sample so the light power is well-defined on the sample.

2.3.1. Resistance vs. Temperature (RT)

Resistance measurements were taken using four probe Lock-in technique using a SR–7625 lock-in amplifier. The current was kept below 100nA, which is low enough to ensure ohmic behavior. In order to minimize noise and decrease losses, the frequency was chosen in the regime 11–33 Hz, where the signal to noise ratio is above 100.

Temperature control were achieved by a Lakeshore–340 controller, wired to a DT-470 thermometer, which is placed on the sample holder, and controls a heater close to the sample.

The sample was heated up to a temperature of 10K and then sweeped down to base temperature while measuring resistance.

For each degree of disorder, R(T) measurements were taken three times: once before the illumination for a reference, second during illumination for monitoring and third after illumination for observing changes.

3. Results

In this work, we present measurements of consecutive stages of one of our samples, *"Sample F1"* achieved by gradual annealing. The initial film was evaporated at an oxygen pressure of $5 \cdot 10^{-5}\ mbar$.

3.1. R(T) measurements

For each stage, R(T) measurements were taken before and after light illumination. Fig. 3.1 illustrates the R(T) curves of the gradual stages of *F1*.

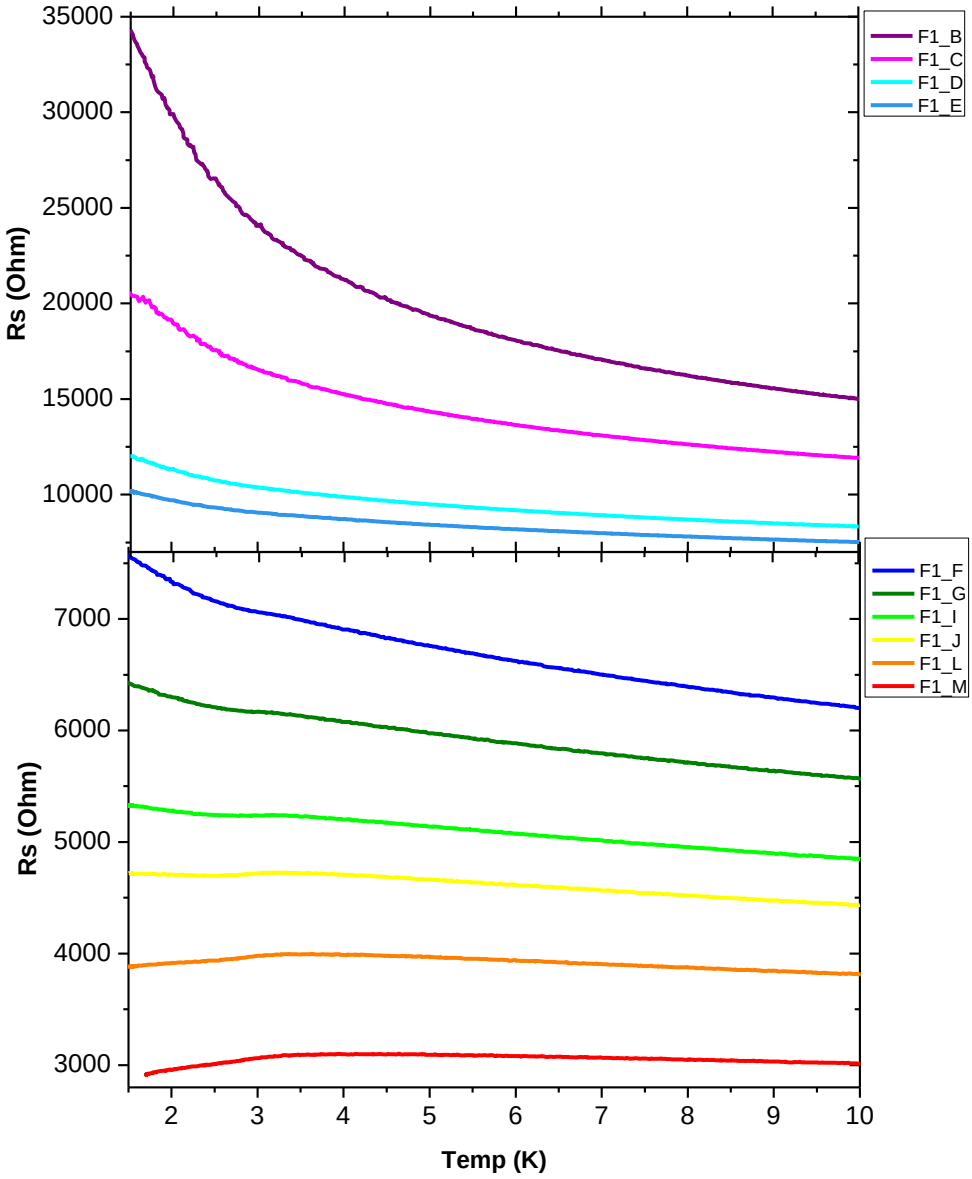

FIG. 3.1: R(T) curves of *F1* in the different stages.

As can be seen, with decreasing disorder, which in our case is expressed by R_{sq} (sheet resistance), the sample crosses over from an insulating state to a SC state. The same data normalized to R(T=10K) are shown in Fig. 3.2.

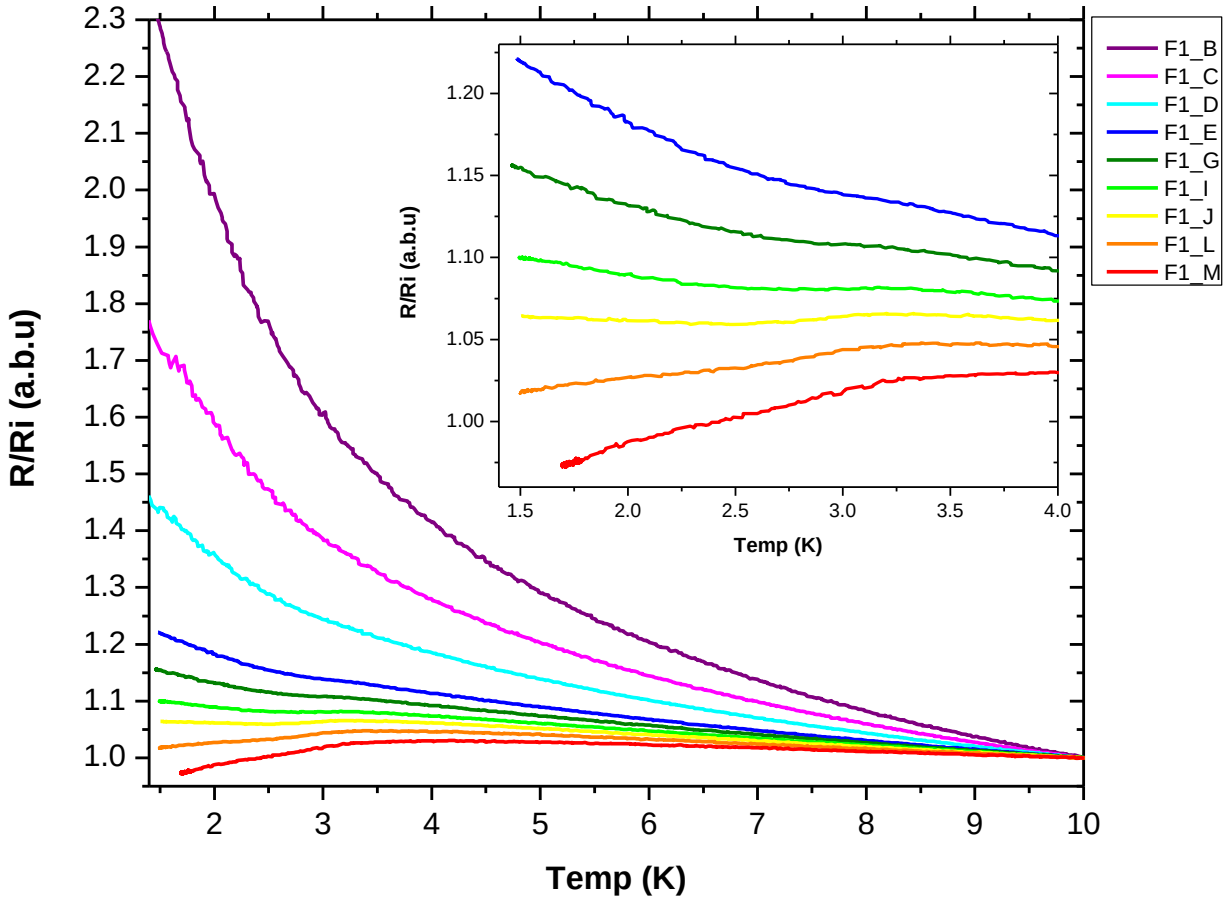

FIG. 3.2: Normalized R(T) curves of *F1*, where each color represents a different stage. *Inset:* Zoom on the SIT regime of the sample.

As shown in the inset, at stage J, the curve exhibits a slight increasing in resistance below 2.5K, while at stage L, the resistance decreases below 2.5K. Hence, the sample crosses the SIT between stages J and L.

In order to check the conductance mechanism in our sample, we plotted the log(R) as a function of $T^{\frac{1}{2}}$ and $T^{\frac{1}{4}}$, for stage B and J of *F1*, which are a strong insulator and a sample close to the SIT respectively. The results are shown in Fig. 3.3.

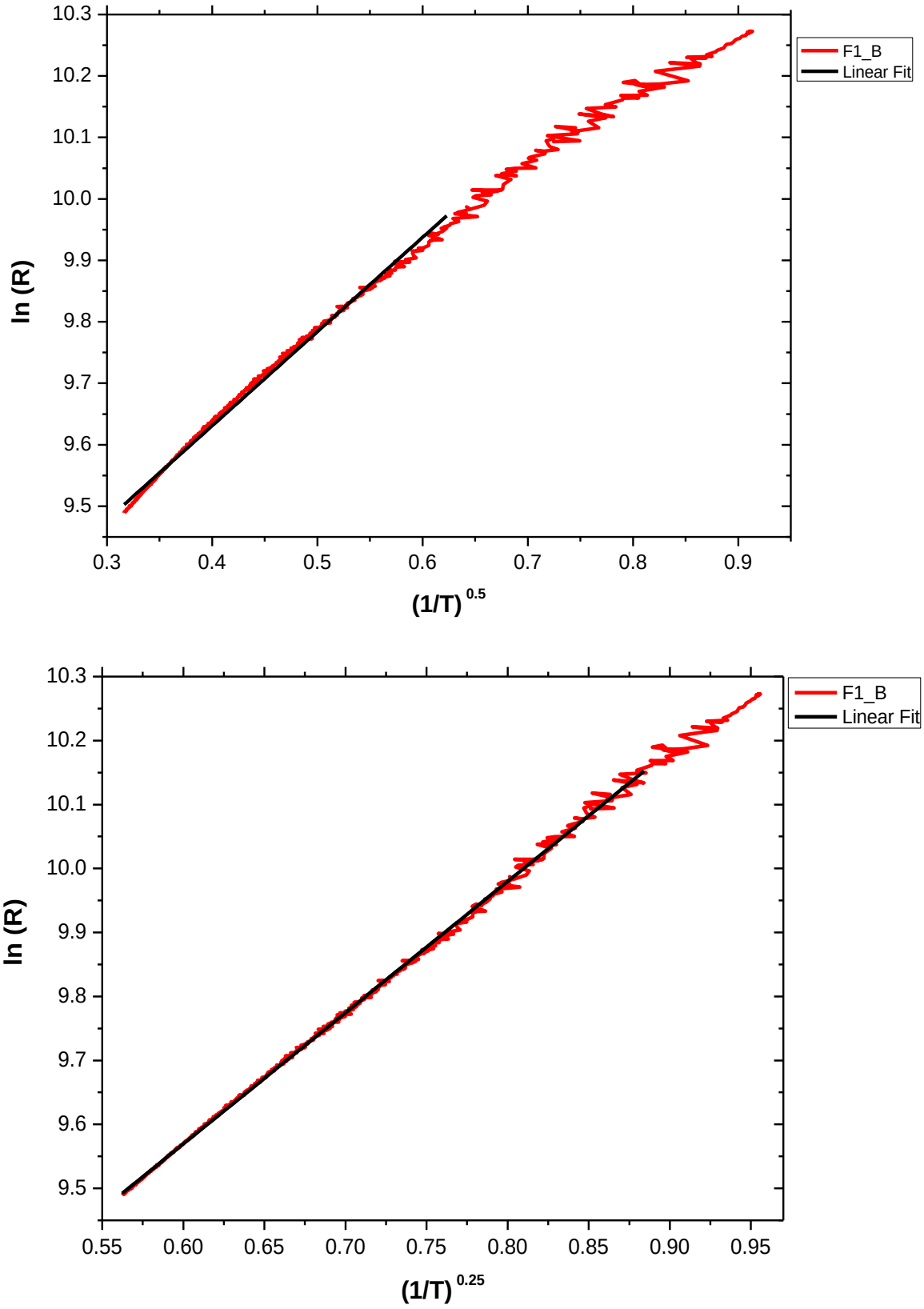

FIG. 3.3: *Top:* Ln(R) as a function of $T^{\frac{1}{2}}$. *Bottom:* Ln(R) as a function of $T^{\frac{1}{4}}$, for stage B of *F1*. *Black line* is a linear fit.

It can be seen clearly that the conductivity behaves in accordance with the Mott VRH mechanism, where the slope of the curve corresponds to $T^{\frac{1}{4}}$, giving a T_0 of 16K.

On the other hand, for stage J, which is slightly above the SIT, it is seen in Fig. 3.4 that log (R) is sub linear with $T^{\frac{1}{4}}$, i.e. the behavior of the conductivity is no longer hopping.

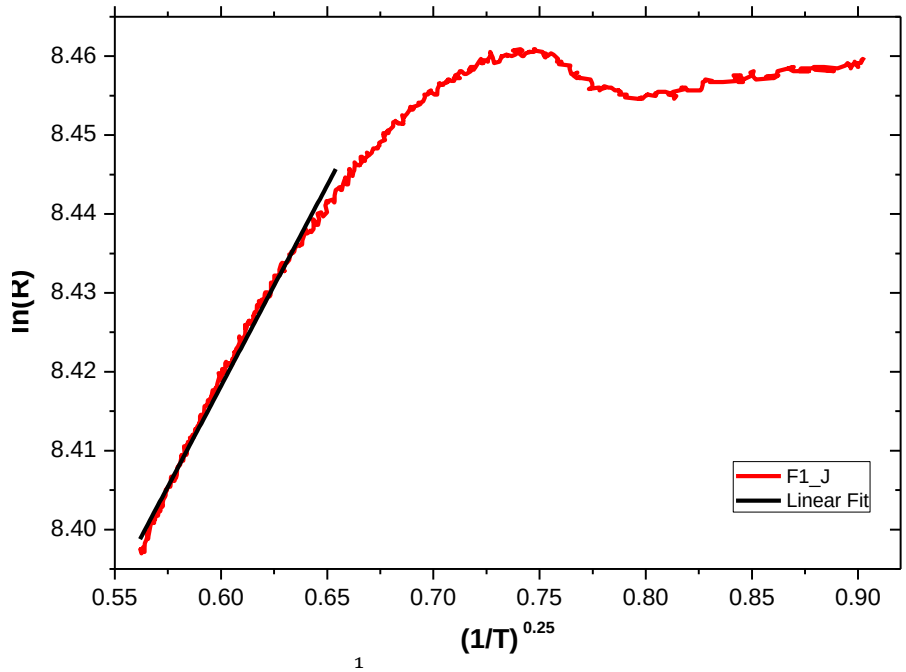

FIG. 3.4: Ln(R) as a function of $T^{\frac{1}{4}}$, for stage J of *F1*. *Black line* is a linear fit.

We also checked dependence on logarithmic temperature, which corresponds to weak localization mechanism but it did not fit. We therefore conclude that these stages are in an intermediate regime between Weak localization and strong localization.

3.2. R(T) after shining Light

As depicted in Fig 3.5, two sets of R(T) measurements were taken for each stage. The first R(T) was taken for a reference before illumination *(whole line)*. Then, the sample was illuminated for 3.5 hours and after turning off the light another R(T) was taken *(scattered line)*. Both curves are normalized where the colors represent different stages.

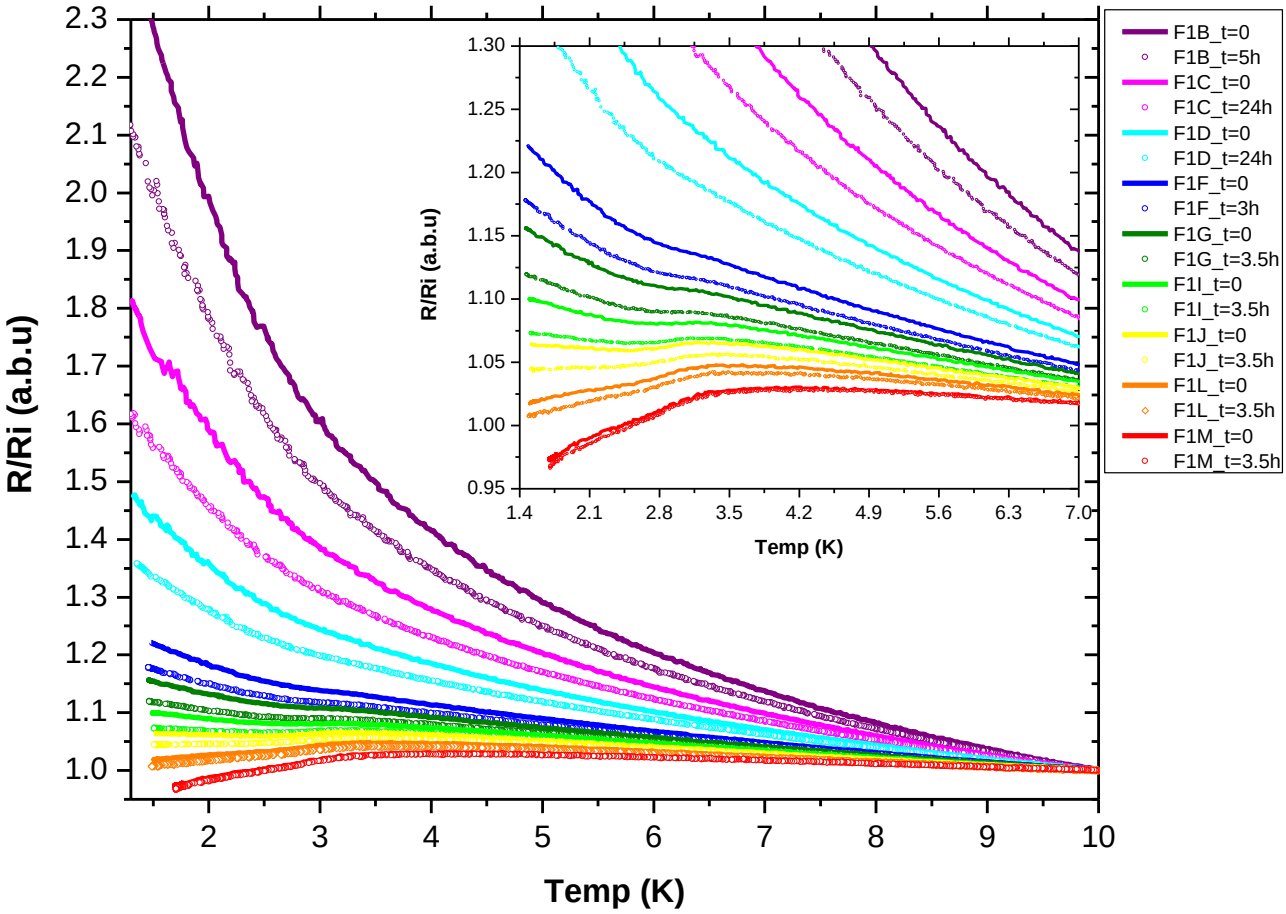

FIG. 3.5: Normalized R(T) curves of *F1*. Each color represents different stage, before illumination *(whole lines)* and after illumination *(scattered)*. *Inset:* Zoom on the curves close to the SIT.

It can be seen in the inset that, as getting close to the SIT, the R(T) measurements of the sample exhibit a 'shoulder', which is consistent with a granular behavior.

In addition, for each stage, whether the sample is an insulator or a superconductor, the resistance decreased due to illumination and did not return to its initial values even after a long time.

A most significant result is presented in Fig. 3.6. The R(T) curve of stage J exhibits insulating behavior *(blue)*, but after illuminating, the sample transits to a superconductor, as shown in the lower R(T) curve *(red)*. **The novelty of this result is that a sample can cross the SIT by just shining light on it**.

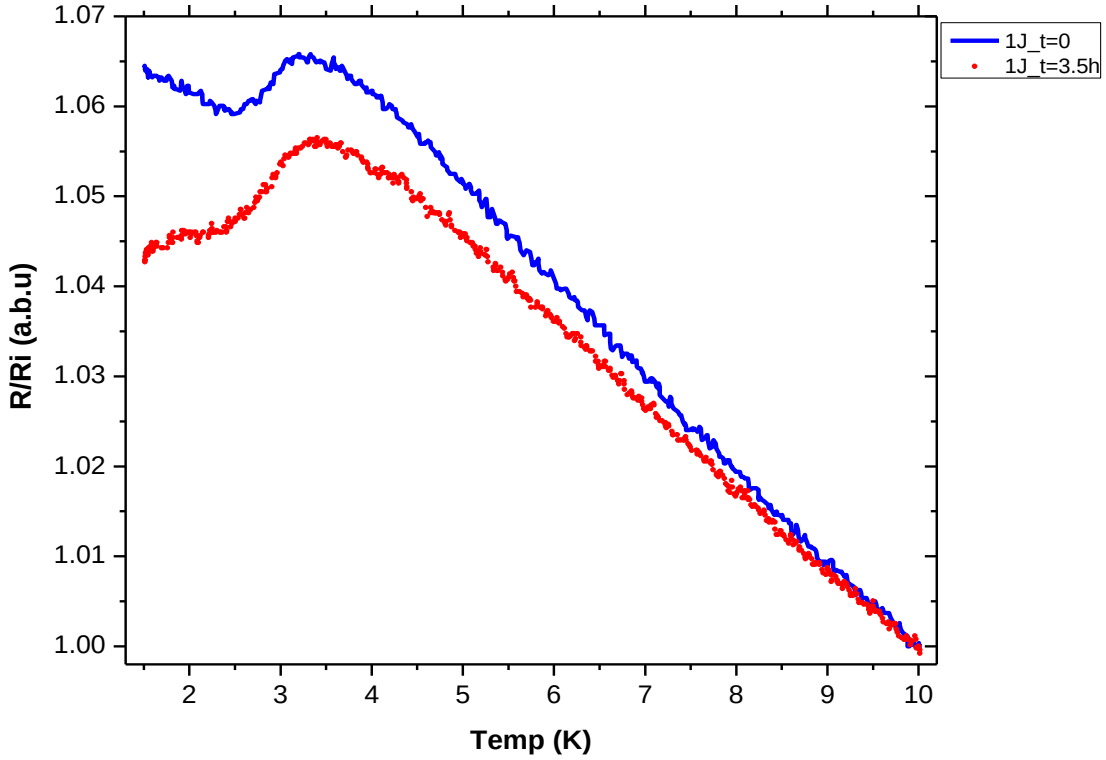

FIG. 3.6: Normalized R(T) curves of stage J of *F1*, before illumination *(blue line)* and after 3.5 hours of illumination *(red dots)*. The upper curve seems to be an insulator while the lower curve seems to be a superconductor.

It should be noted that in our optical cryostat, we are limited to a temperature of 1.3K, so the low temperature trends are not available. We assume that an extrapolation to zero temperature will continue the tends that if the resistance increases the sample is an insulator at T=0, and if the resistance decreases the sample is SC.

3.3. Time dependent conductivity

In order to examine evolution of electronic properties while shining light, time measurements were taken during the illumination. Fig. 3.7 presents the $\sigma(t)$ measurement of stage G at a temperature of 1.45K. First, a base line was determined for 250 seconds. Then, at t=250s the light was turned on and remained open until t=12300 sec.

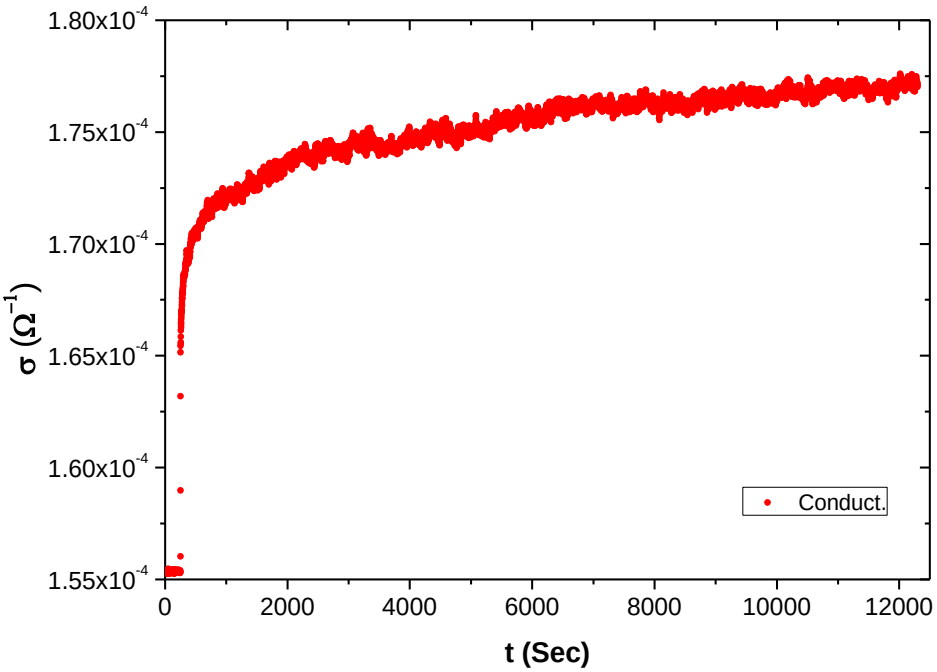

FIG. 3.7: $\sigma(t)$ measurement of the illumination process. The light was turned on at t=250s and turned off at t=12300s.

It turns out that the time dependence process contains two contributions. The first is a fast increase in conductance, which occurs in the first few seconds. The second is a slow excitation that follows a logarithmic behavior, as shown in Fig. 3.8.

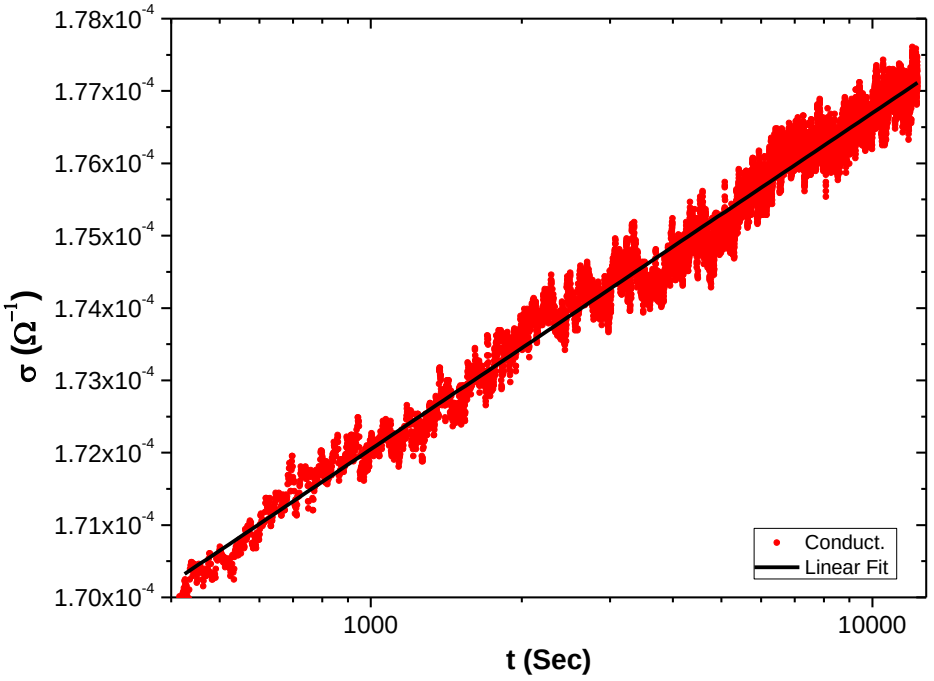

FIG. 3.8: The slow excitation part of Fig. 3.7 in log scale. *Black line* represents a linear fit.

In Fig. 3.9, the conductivity vs. time is presented for different stages from insulator to superconductor. The conductivity is normalized to the initial value before illumination (reference value). It is seen that for stage G, in which the sample is an insulator, the initial jump in conductivity is large and the second part exhibits a large logarithmic slope. With decreasing sample resistance, the initial jump decreases, and the slope at longer times becomes smaller.

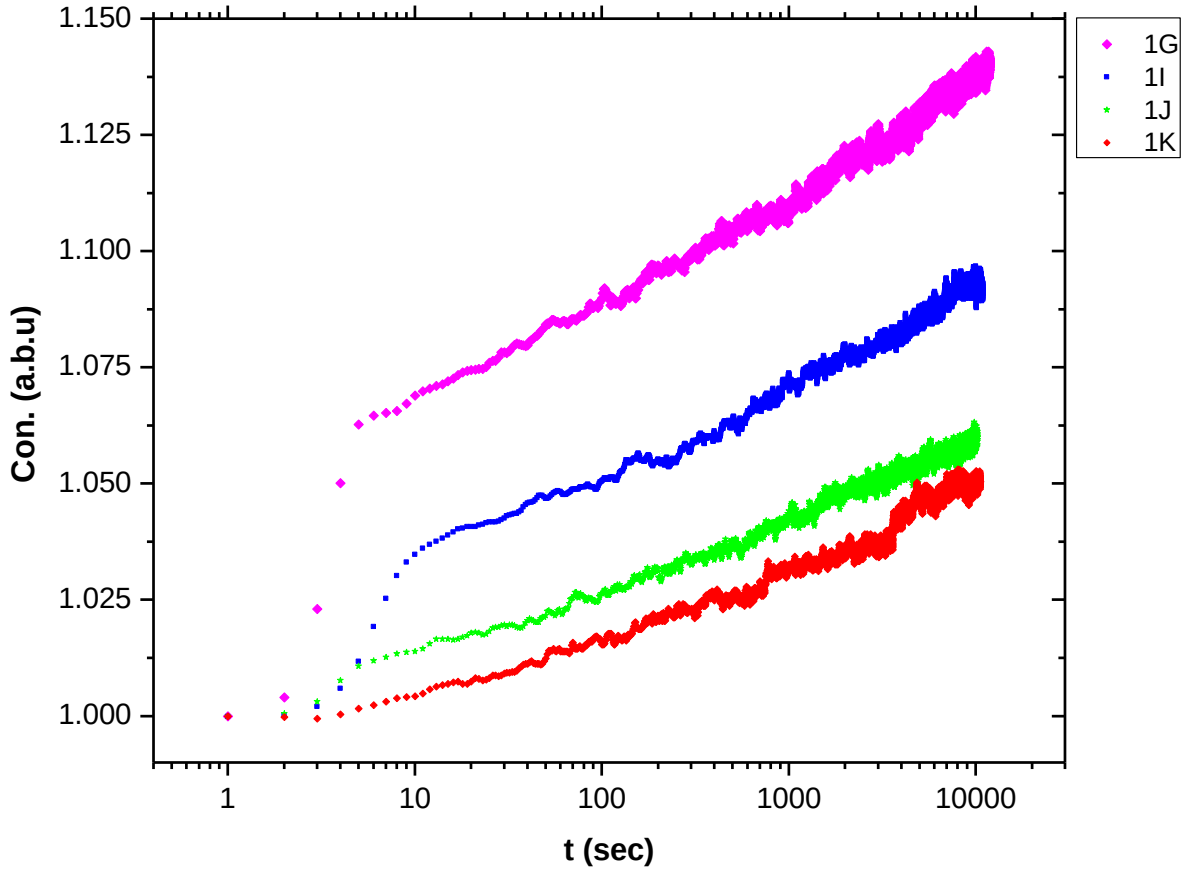

FIG. 3.9: Conductivity vs. log(t) of the illumination process for different stages of *F1*.

We also measured time dependent conductivity after the illumination was turned off in order to examine the relaxation back to equilibrium. Fig. 3.10 presents the $\sigma(t)$ measurement of stage C on a logarithmic scale at a temperature of 1.35K. The measurement starts about 100 sec after turning off the light due to experiment limitations.

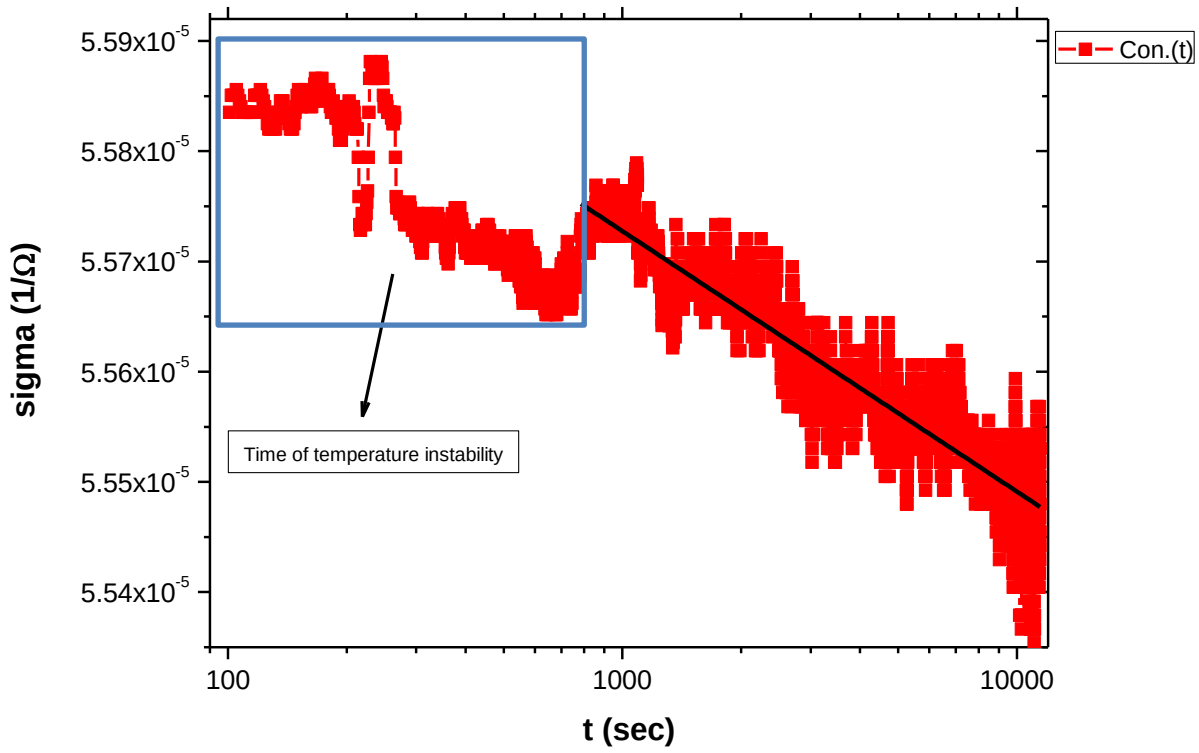

FIG. 3.10: Conductivity vs. log(t) of stage C after turning off the light. The marked area is the regime in which temperature was unstable. *Black line* represents a linear fit.

It is seen that the curve follows a logarithmic behavior as well. It should be noted that at small times (*marked area*), the curve is very noisy due to temperature instability.

A natural explanation for the changes in conductivity could be that the laser beam causes an irreversible morphology change in the sample. In order to check this possibility, we performed R(t) measurements of the sample during illumination at T=299K (room temp.). The results are shown in fig 3.10. The laser was turned on at t=400s and turned off at t=2000s, while the temperature was measured simultaneously in order to ensure that it does not change with illumination. Fig. 3.11 shows both R(t) *(top)* and T(t) *(down)*. The resistance has fluctuations of ±2Ω on a background of 4.236K (0.05%) during the whole

experiment, while at the same time the temperature is fairly stable with oscillation of 0.007%. Hence, it can be concluded that no structural changes are created in the sample as a consequence of shining the light.

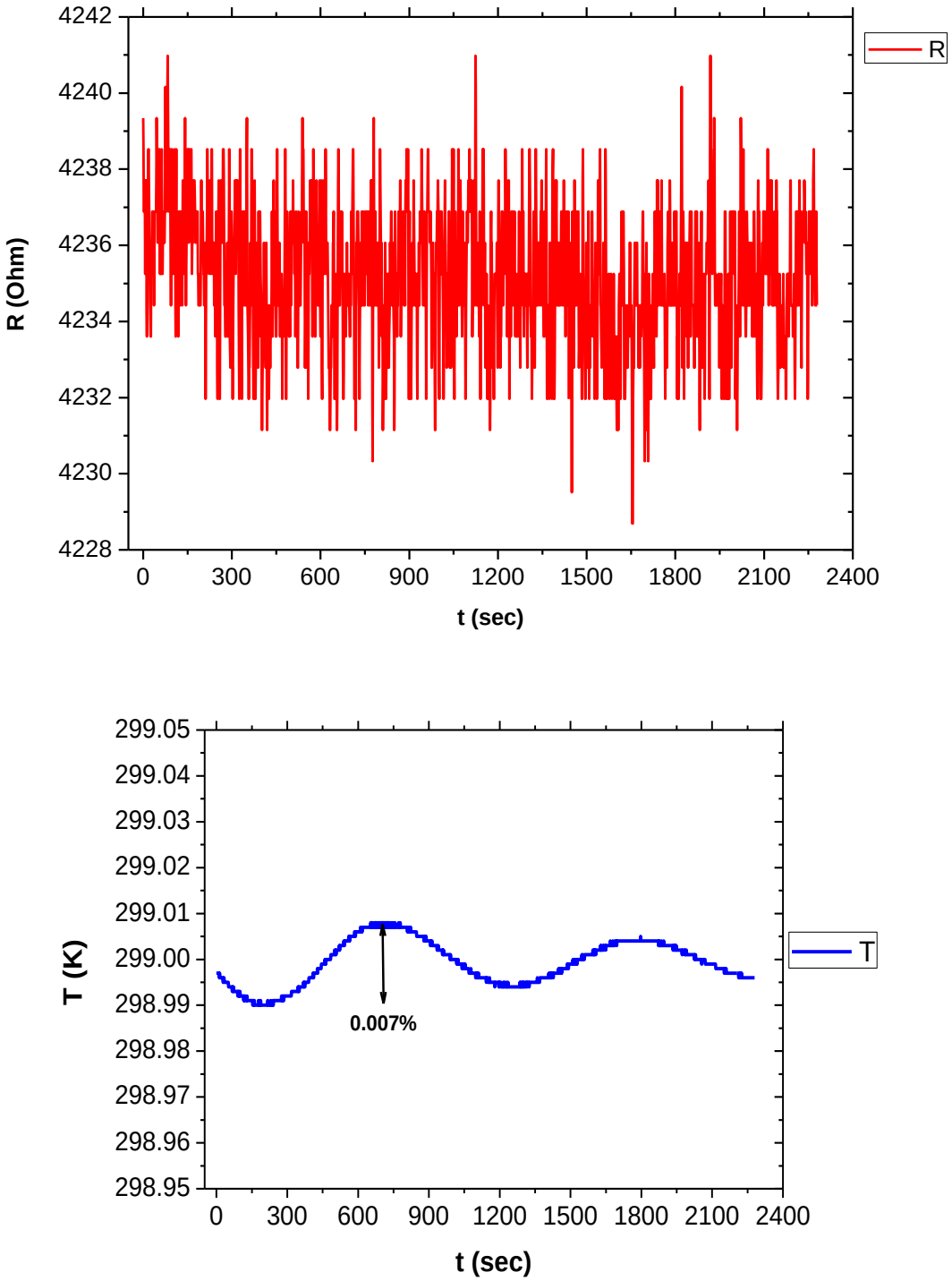

FIG. 3.11: *Top:* R(t) curve at 299K which shows no changes in resistance during illumination. *Bottom:* T(t) measurement which was taken simultaneously in order to ensure that the temperature is stable.

Furthermore, a comparison between the R(T) measurement which was taken before illumination and after illumination shows that the curves merge at a temperature of about 180K approximately, as presented in Fig. 3.12, providing further evidence that no irreversible changes occur.

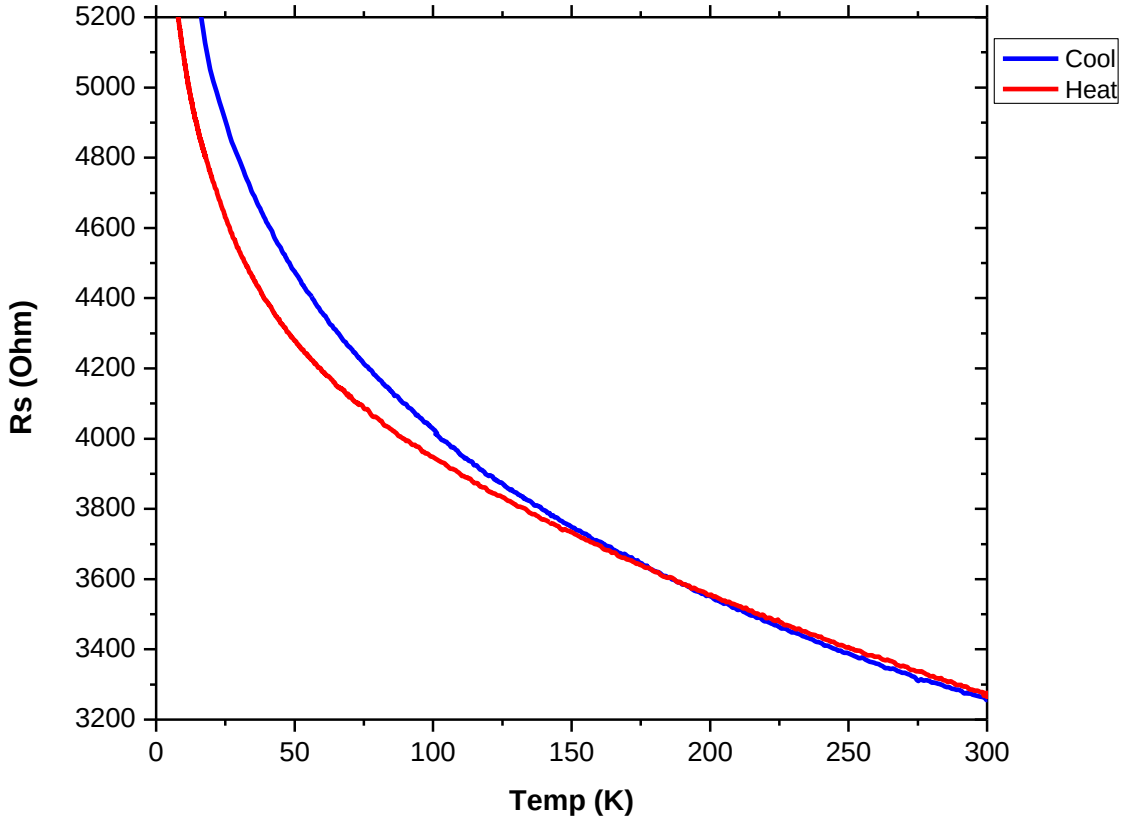

FIG. 3.12: R(t) curves of cooling down *(blue line)* and heating back *(red line)* show merging at 180K approximately. These curves were taken for stage H of *F1*.

These two results refute the possibility of light induced topological changes and demonstrate that illumination affects the electrical configuration of the sample and not its morphology.

4. Discussion

As noted above (1.2.3), a-InO films belong to a type of metals, which are morphologically homogeneous but possess granular behavior, manifested by SC regions separated by a normal state insulating sea. Moreover, experiments indicate that granularity exists even in the insulating side of the SIT and is similar to the granularity in the SC side [29].

The R(T) measurements which are presented in Fig. 3.5 exhibit a 'shoulder' that is consistent with granular behavior. On the other hand, an AFM image shows continuous morphology. Combining these two facts provides an additional evidence for the existence of electrical granularity.

The novel result is the so called "light induced SIT", in which our sample, which is an insulator initially, crosses the SIT and becomes a superconductor, only by shining light on it, and persists for a relatively long time with a very slow relaxation.

To explain out result, we suggest a model for the conductivity.

4.1. Qualitative model for "long lived" conductivity

Perhaps the main finding is the so called "long lived conductivity" phenomenon. It turns out that when shining light on the sample, the conductivity jumps to a higher value and remains at this value even after turning off the light.

This modification is manifested as a significant reduction in resistance on the insulating side. In the SC regime, in addition to reducing normal state resistivity, it improves superconductivity reflected in the raising of T_c, where the influence of light decreases as the sample becomes more superconductor, as shown in Fig. 4.1.

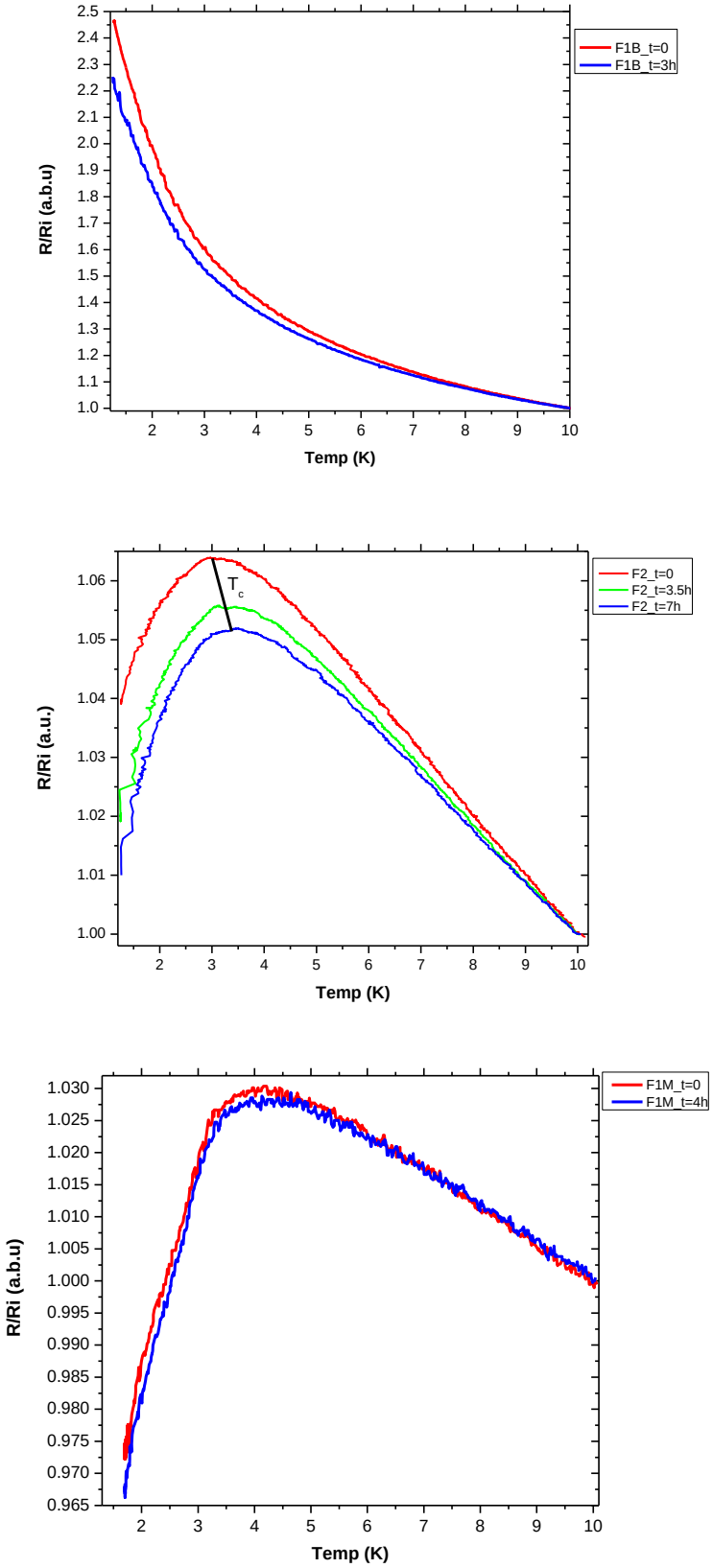

FIG. 4.1: Normalized R(T) curves before *(red line)* and after *(blue line)* illumination. *Top:* Stage B of *F1*('strong' I), *Middle:* Sample *F2* ('weak' SC). *Bottom:* Stage M of *F1* ('stronger' SC).

To understand the results, we suggest the following qualitative model:

When light is incident on the sample, all electrons are excited instantly to higher energy levels and Cooper pairs are broken, resulting in a modification of the electrical configuration of the system. Consequently, when the main contribution to conductivity is that of the insulating regions, the resistance decreases due to the excited electrons, and contrarily, when the main contribution is of the superconducting grains, the resistance increases due to breaking of Cooper pairs by light.

Apparently, the high energy levels are meta-stable, so when turning off the light the electrons of the insulating regions remain excited for a long time, thus keep contributing to increased conductivity, while the electrons in the SC regions recombine immediately as Cooper pairs. This new configuration of SC grains with a sea of long live excited electrons in between strengthens the coupling between the grains and leads to a decrease in resistance.

Fig. 4.2 shows two sets of R(T) curves. The first (*blue lines*) were taken as a reference before illumination and the second (*red lines*) were taken during the illumination. It can be seen that for stage C (*top graph*), in which the sample is a 'strong' insulator, the resistance is significantly reduced during illumination. For stage M (*bottom graph*), in which the sample is a superconductor, above T_c, there are no SC regions thus the contribution is of the insulating regions thus the resistance decreases. However, below T_c, where a global phase coherence is generated between the SC grains, the main contribution is now of the SC regions thus the resistance increases, due to breaking of Cooper pairs by light.

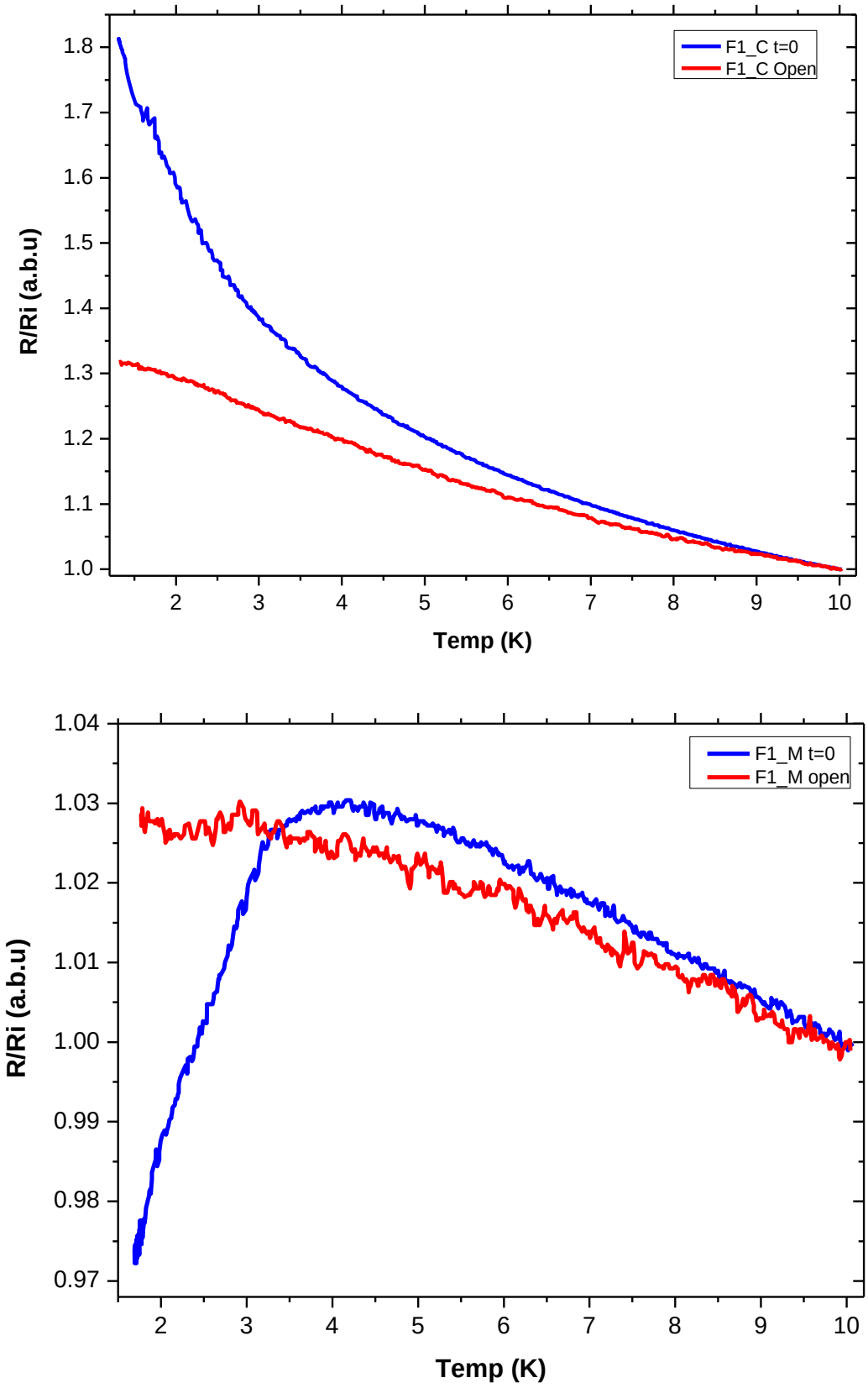

FIG. 4.2: Normalized R(T) curves before *(blue line)* and during *(red line)* illumination. *Top:* Stage C, which is an insulating, *Bottom:* Stage M, which is a SC.

Another way to think of this is by percolation. The light changes the resistance of the network by adding electrons to the backbone cluster and creating more paths, which enhance the correlation between the SC grains, resulting in decrease of the critical resistor.

The above process leads to the most significant finding, which is a new type of SIT. It occurs in stage J, in which the light affects the insulating regions so that a correlation between the SC grains is created, resulting in phase transition from an insulator to a superconductor. In other words, a sample, which is expected to be an insulator with infinite resistance at zero temperature, turns to a superconductor with zero resistance at zero temperature, only by illumination.

The strength of this phenomenon must depend on the size of the normal regions, which in turn depends on the degree of disorder. Deep in the insulating side, where the SC islands are small and the normal regions in between are fairly large, the influence of illumination is stronger. With decreasing the level of disorder, the influence of light is reduced due to growth of the SC regions and decrease in resistance of the normal regions, down to negligible values deep in the SC side. It can be seen from Fig. 4.1 that while in stage B, the light causes a significant reduction of resistance of about 8%, in stage M the change is negligible (less than 1%).

Fig. 4.3 shows the percentage of resistance decrease, or ΔR, for each stage as a function of R_{sq} (which is equivalent to disorder level) at a temperature of 10K. ΔR is extracted from the normalized R(T) curves by:

$$\Delta R(\%) = 100\left(1 - \frac{R_f(1.5K)}{R_i(1.5K)}\right)$$

In the insulating side, the curve shows linear behavior. When approaching the vicinity of the QCR, ΔR drops faster until stage L *(marked with arrow)*, in which the sample becomes a macroscopic superconductor.

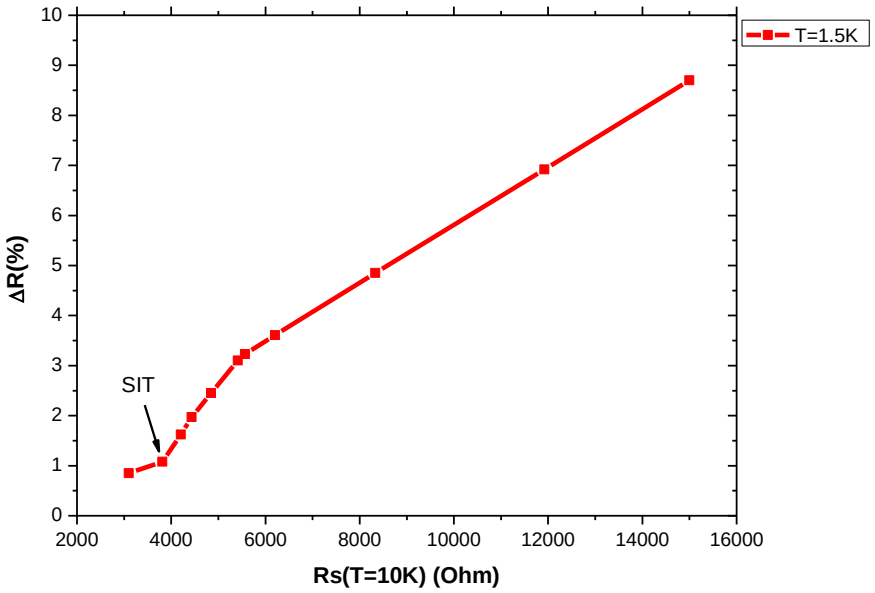

FIG. 4.3: Δ*R* in percentage as a function of R_{sq}. In stage L *(marked with arrow)*, the sample becomes a superconductor after crossing the SIT.

So, what can be the origin of such 'long lived' conductivity?

As discussed above in 1.4, InO_x films have been shown to possess an electron glassy behavior. Indeed, the work done by Z. Ovadyahu [28] shows a glassy behavior in InO_x film, deep in the insulating side. He also claims that glassy behavior persists only in a case of strong localized systems with resistance per square of above 30K.

However, in the samples close to the SIT the situation may be different. In our measurements, glassy behavior may be observed, due to the unique morphology of SC and insulating regions. Indeed, the logarithmic dependence of the R(t) measurements are consistent with EG behavior.

In conclusion, our work presents a novel way to control the SIT in disordered films non-invasively (without changing its morphology), while as opposed to other external tuning parameters, such as magnetic field, the impact on the system is steady even after cessation of irradiation of light, due to a glassy behavior. It also opens a window for a new field of experimentation, which may reveal more about the physical behavior of such disordered films.

4.2. Justification of excitation

It should be noted that our working premise is that light affects a large part of the system due to observation of large changes in the resistance of the films. One should check if this is the situation in our experiment.

Fundamentally, the total amount of electrons in a medium is given by:

(1.12) $$N_e = n_e \cdot V$$

where n_e is the number of electrons to a volume unit and V is the volume. In InO_x materials, n is of the order of $10^{21}\ cm^{-3}$. With dimensions of $0.64\text{mm} * 0.78\text{mm} * 30\text{nm}$, the volume of the sample is about $1.5 \cdot 10^{-9}\ cm^3$. Hence, the total amount of electrons in the sample is about $2 \cdot 10^{12}$.

On the other hand, the power of the laser is 6mW. Following the equation:

(1.13) $$P = \frac{E}{s} = n_{ph} \cdot E_{ph}$$

where n_{ph} is the number of photons per second and E_{ph} is the photon energy. For helium-neon laser E_{ph} is 1.96eV. Using these values yields $2 \cdot 10^{16}$ photons per second, which are three orders of magnitude larger than N_e.

This calculation is approximate and does not take into account other factors such as efficiency, absorption and losses, but the intensity should be enough to support the above assumption.

5. Conclusions

InO films belong to a unique type of systems that undergo the SIT, which exhibit granular behavior despite having a continuous morphology. This granularity is manifested by SC islands surrounded by an insulating sea due to electrical localization.

Deep in the insulating side, experiments have shown an existence of an electron-glassy behavior, which is characterized by a slow relaxation after pushing the system out of equilibrium.

In our work, we investigated the influence of light on sets of samples characterized by different degrees of disorder from a deep insulating state to a superconducting state, achieved by thermal annealing. For each stage, R(T) was first measured, after which we shone light for few hours and then turned off the light and took another R(T). Conductivity as a function of time was measured during the whole process.

We find that light causes a reduction in resistance, which possesses a logarithmic behavior with time. After turning off the light, this low resistance state persists for a long time with a very slow relaxation that is also exhibits a logarithmic behavior. Our experiments confirm that the light does not change the morphology of the samples but rather the electronic properties.

One of the outcomes is a "light induced SIT", in which a sample with a degree of disorder which is slightly above the SIT, crosses the SIT and becomes a superconductor, by just shining light on it.

Combining all results together we suggested a qualitative model, in which the insulating regions between SC grains behave as an EG. By shining light on the system, the "normal" electrons are excited to higher "meta-stable" energy levels, resulting in a conductivity. This improvement of conductivity leads to an enhancement of the coupling between SC islands, resulting in pushing the system towards the SC side.

Our work is innovative by the fact that the system is excited by illumination. It adds a new dimension of measurements, which not only provides further evidence for electrical granularity but also presents qualitative information on the characteristics of the material in between these SC grains, and may lead to a new type of SIT.

In conclusion, we conducted a pioneering work in the field of optical research of disordered films that has significant impact on the investigation of their physical behavior. It also opens a window for additional measurements, which can provide more information about the properties of these films.

Further plans

Our work opens a window to a new field of research. In this section, we suggest some additional experiments, which may reveal further information about the properties of the films.

1. Sufficiently low temperatures

As mentioned, our optical cryostat is limited to a base temperature of 1.3-1.6K. Hence, the significant result of crossing the SIT by just shining light on the sample is not very clear and requires significant extrapolation to zero temperature.

In order to obtain more explicit results, one should conduct this experiment at sufficiently low temperatures. This requires a new experimental set-up.

2. Glassy behavior

As shown, both processes of excitation and relaxation of conductivity are characterized by a logarithmic dependence, which supports the conjecture that the insulating regions behave as an electron glass.

In order to further check this conjecture, a suitable experiment is a measurement of other characteristic of the electron glass such as the so called "memory dip". Based on the fact that an EG system retains a memory of the

last state at which it was allowed to equilibrate, applying a gate voltage on a system for a long time and then performing fast of gate voltage scans presents a dip in the conductance versus gate voltage curve. An existence of such phenomenon in our films close to the SIT will strengthen the model and provide more information about the glassy behavior of the film.

3. Time dependent transmission

Heretofore, most of our experiments deal with the electrical properties of the films. What may also be important and interesting in the context of our research are the optical properties, such as transmission and absorption of light through the sample.

We showed that shining light on the sample leads to a jump in conductance, which consists of two contributions, a fast increase and a slow excitation. We postulate that the initial jump occurs as a result of fast excitation of electrons to high energy levels after which, the excitation decays slowly with time due to electron-electron interactions leading a logarithmic tail. Thus, measuring the transmission and absorption of the film as a function of time, may provide further insight into the processes that govern the electronics of the normal region between SC islands.

6. Bibliography

[1] P. W. Anderson, *Phys. Rev.*, vol. 109, p.1492 (1958)

[2] N. Mott, *Phil. Mag.*, vol. 19, p.835 (1969)

[3] A. L. Efros and B. I. Shklovskii, *J. Phys. C*, vol. 8 (1975)

[4] B. Suki, *Frontiers in physiology*, vol. 94, p. 3 (2012)

[5] V. K. S. Shante and S. Kirkpatrick, *Advances in Phys.*, vol. 20, p. 325 (1971)

[6] V. Ambegaoker, B. I. Halperin and J. S. Langer, *Physical Review*, vol. 4, p. 2612 (1971)

[7] J. H. Davies, P. A. Lee and T. M. Rice, *Phys. Rev. Lett.*, vol. 49, 758761 (1982)

[8] G. Parisi and F. Sciortino, *Nature materials*, vol. 12, p.94 (2013)

[9] Z. Ovadyahu, *Physical Review. B*, vol. 73, 214208 (2006)

[10] T. Grenet, J. Delahaye, M. Sabra and F. Gay, *Eur. Phys. J. B*, vol. 56, p.183 (2007)

[11] T. Havdala, A. Eisenbach and A. Frydman, *"Ultra-slow relaxation in discontinuous-film based electron-glasses"* (2012)

[12] K. Matan, R. B. Willliams et al., *Phys. Rev. Lett.*, vol. 88, 76101 (2002)

[13] A. Eisenbach et al., *Phys. Rev. Lett. B.*, vol. 117, 116601 (2016)

[14] Z. Ovadyahu, "*Slow relaxations and non-equilibrium dynamics"*, p.625, (2003)

[15] P. W. Anderson, *J. Phys. Chem. Solids*, vol. 11, p. 26 (1959)

[16] A. Abrikosov and L. Gor'kov, *Sov. Phys. JETP*, vol. 9, p. 220 (1959)

[17] D. B. Haviland, Y. Liu, and A. M. Goldman, *Phys. Rev. Lett.*, vol. 62, p. 2180 (1989)

[18] V. F. Gantmakher et al., *JETP letters* 71 11, 473 (2000)

[19] T. Baturina and V. Vinokur, *Annals of Physics*, vol. 331, p. 236 (2013)

[20] A. Frydman, *Physica c*, *v*ol. 391, p.189 (2003)

[21] S. Maekawa and H. Fukuyama, *J. Phys. Soc. Jpn.*, vol. 51, p.1380 (1981)

[22] H. Takagi, R. Souda and Y. Kuroda, *Progress of Theoretical Physics*, vol. 68, p. 426 (1982)

[23] A. Finkel'shtein, *JETP*, vol. 45, p. 46 (1987)

[24] Matthew P. A. Fisher, Peter B. Weichman, G. Grinstein, and Daniel S. Fisher, *Phys. Rev. Lett B.*, vol. 40, p.546 (1989)

[25] R. P. Barber, L. M. Merchant et al., *Phys. Rev. Lett B.*, vol. 49, p.3410 (1994)

[26] A. Ghosal et al., *"Role of Spatial Amplitude Fluctuations in Highly Disordered s-Wave Superconductors"* (1998)

[27] K. Bouadim, Y. L. Loh, M. Randeria and N. Trivedi, *Nature Physics*, vol. 7, p. 884 (2011)

[28] D. Sherman, G. Kopnov, E. Farber, D. Sahar and A. Frydman, *J. Supercond. Nov. Magn.*, vol. 26, p. 1473 (2013)

[29] D. Shahar and Z. Ovadyahu, *Physical Review. B*, vol. 46, p. 10917 (1992)

תקציר

מעבר על מוליך– מבודד (SIT) בשכבות דקות הינו תופעה חשובה, אשר נמצאת בחוד החנית של המחקר במצב מוצק. תופעה זו נחשבת לדוגמא קלאסית של מעבר פאזה קוונטי (שאיננו תלוי בטמפרטורה) בו מערכת מבודדת הופכת לעל מוליכה בטמפרטורה אפס. עיקר המחקר העוסק ב-SIT כיום מתמקד באזור הקריטי של המעבר (QCR), מאחר ובתחום זה התנהגות החומר איננה טריוויאלית. למרות המאמצים הרבים, הן בתחום התיאורטי והן בתחום הניסיוני, חלק ניכר מהפיזיקה עדיין לא ברור, בעיקר ההתנהגות של החומר בצד המבודד.

אחד המודלים המוצעים על מנת להסביר חלק מהתופעות שנצפו, נקרא "Emergent granularity", אשר מצביע על התנהגות גרעינית של החומר למרות שמורפולוגית הוא רציף. מבחינה אלקטרונית, ניסויים הראו כי הגרעיניות מתבטאת כאיים של על מוליכות המוקפים באזור מבודד. אינדיום אוקסיד, אשר עובר את מעבר הפאזה הנ"ל, הוא דוגמא לסוג כזה של מערכות.

מלבד זאת, ניסויים שנעשו בדגמים "מבודדים חזקים" (הרחק מהמעבר) הראו קיום של זכוכית אלקטרונית (Electron glass) המתאפיינת ברלקסציה מאוד איטית כתגובה להוצאת המערכת משיווי משקל.

בעבודה זו, אנו מציגים ניסוי שלא נעשה עד כה, הבוחן את ההשפעה של הארה על דגמי אינדיום אוקסיד ברמות שונות של אי-סדר, ממבודד חזק ועד לעל מוליך, כאשר כל מעבר מרמת אי סדר אחת לשנייה מתבצע ע"י הרפיה תרמית. בכל שלב, מדדנו תחילה את ההתנגדות כתלות בטמפרטורה. לאחר מכן, הארנו את הדגם לכמה שעות, ואז, לאחר כיבוי האור, מדדנו פעם נוספת את ההתנגדות כתלות בטמפרטורה. כמו כן, מדידה של ההתנגדות כתלות בזמן בוצעה לכל אורך התהליך.

הממצאים העיקריים הם כדלקמן:

1. האור גורם לעלייה במוליכות, כאשר התלות בזמן היא לוגריתמית.
2. לאחר כיבוי האור, המוליכות לא חוזרת לערכה ההתחלתי אלא נשארת לזמן ארוך ודועכת מאוד לאט כאשר גם כאן התלות בזמן היא לינארית.
3. השיפור במוליכות גורם להגדלת הקורלציה בין האיים העל מוליכים, מה שדוחף את המערכת אל הצד העל מוליך. אחד הממצאים המעניינים שהתקבלו כתוצאה מכך הוא "מעבר על מוליך– מבודד עקב הארה", בו דגם הנמצא בצד המבודד, מעט מעל המעבר, חוצה אותו והופך לעל מוליך ע"י הארה עליו בלבד.
4. האור אינו משנה את המורפולוגיה של החומר אלא רק את התכונות האלקטרוניות.

על סמך התוצאות הנ"ל, אנו מציעים מודל, לפיו האזורים המבודדים שבין האיים העל מוליכים מתנהגים כזכוכית אלקטרונית. כאשר מאירים על המערכת, האלקטרונים

באזורים אלו מעוררים לרמות אנרגיה גבוהות "מטה-סטבילויות", מה שמאפשר לאיים העל מוליכים להגדיל את הקורלציה ביניהם וגורם לשיפור המוליכות. בקרבת המעבר, העלייה הזו במוליכות גורמת להיווצרות קוהרנטיות בפאזה העל מוליכית ולהפיכתו של הדגם ממבודד לעל מוליך. בצד העל מוליך, השיפור מתבטא בעלייה של טמפרטורה הקריטית של הדגם.

עבודה זו מוסיפה מימד חדש של מדידות, שלא רק מספק ראיה נוספת ל-emergent granularity, אלא גם מציגה מידע איכותי על טיב החומר שבין הגרגירים העל מוליכים, ומוביל לסוג חדש של מעבר על מוליך– מבודד. לעבודה זו ישנה השפעה רבה בחקירה של על מוליכים לא מסודרים והיא פותחת חלון למדידות נוספות שיכולות לספק עוד מידע על התכונות הפיסיקליות של חומרים אלו.

עבודה זו נעשתה בהדרכתו של

פרופ׳ אביעד פרידמן

מן המחלקה לפיסיקה של אוניברסיטת בר-אילן

אוניברסיטת בר-אילן

המחלקה לפיסיקה

מעבר על מוליך – מבודד על ידי הארה

נריה אושרי

מוגש כחלק מהדרישות לשם קבלת תואר מוסמך
במחלקה לפיזיקה של אוניברסיטת בר אילן

רמת גן, ישראל תשע״ז

אוניברסיטת בר-אילן

המחלקה לפיסיקה

מעבר על מוליך – מבודד
על ידי הארה

נריה אושרי

מוגש כחלק מהדרישות לשם קבלת תואר מוסמך
במחלקה לפיזיקה של אוניברסיטת בר אילן

רמת גן, ישראל תשע״ז